This is the authors' post-print copy of a manuscript for Phytochemistry Reviews.

Please cite as:

Şöhretoğlu D, Yüzbaşıoğlu Baran M, Arroo R, Kuruüzüm-Uz A.

Recent advances in chemistry, therapeutic properties and sources of polydatin.

Phytochemistry Reviews (2018) https://doi.org/10.1007/s11101-018-9574-0

Recent advances in chemistry, therapeutic properties and sources of polydatin

Didem Şöhretoğlu[1*], Merve Yüzbaşıoğlu Baran[1], Randolph Arroo[2] & Ayşe Kuruüzüm-Uz[1]

[1] Hacettepe University, Faculty of Pharmacy, Department of Pharmacognosy, Sıhhiye, 06100, Ankara, Turkey

[2] De Montfort University, Leicester School of Pharmacy, The Gateway, Leicester, LE1 9BH, United Kingdom

* Corresponding author:

Hacettepe University, Faculty of Pharmacy, Department of Pharmacognosy, Sıhhiye, 06100, Ankara, Turkey

Tel: +903123051089

Fax:+903123114777

 E-mail: didems@hacettepe.edu.tr

Abstract

Polydatin (PLD), the 3-*O*-*β*-glucopyranoside of the well-known stilbenoid compound resveratrol, is a major compound of *Fallopia japonica* (Houtt.) R. Decr. (Japanese knotweed), which is widely used in traditional Chinese medicine to treat infection, inflammatory diseases and circulatory problems. It has shown a wide range of biological activities including anti-inflammatory, anti-oxidant, anti-cancer, neuroprotective, hepatoprotective, nephroprotective and immunostimulatory effects. Although resveratrol has similar beneficial effects, its low bioavailability has remained a problem. Glycosylation increases solubility of resveratrol in an aqueous environment, thus improving its bioavailability. This has led to a growing interest in PLD. Promising results obtained from bioactivity studies have boosted an intense research on this compound. The aim of this review is to give a comprehensive overview of the botanical sources, pharmacology, biosynthesis, biotechnological production, and bioactivities of PLD, and to discuss clinical studies on this compound.

Abbrevations

Aβ	Amyloid β
ABTS	2,2'-Azino-bis(3-ethylbenzthiazoline-6-sulfonic acid
AMPK	AMP-activated protein kinase
ALT	alanine aminotransferase
AST	aspartate aminotransferase
Bax	Bcl-2-associated X protein
Bcl-2	B-cell lymphoma-2
BUN	blood urea nitrogen
CAT	Catalase
CC	column chromatography
COX-2	Cyclooxygenase-2
CPC	centrifugal partition chromatography
DPPH	2,2-Diphenyl-1-(2,4,6-trinitrophenyl)hydrazyl
EC	Endothelial cell
ERK	extracellular signal regulated kinase
GC	gas chromatography
GSH-Px	glutathione peroxidase
GSH	Glutathione
GR	glutathione reductase
HO-1	Heme oxygenase 1
HSCCC	high-speed counter-current chromatography
HSP	Heat shock protein
IBS	irritable bowel syndrome
ICAM	Intercellular Adhesion Molecule 1
ICH	The International Council for Harmonisation
Ig	Immunoglobulin
iNOS	Inducible nitric oxide synthase
I/R	Ischemia/Reperfusion
JNK	Jun N-terminal kinase
IL	Interleukin
IRAK	interleukin-1 receptor-associated kinase
LDH	lactate dehydrogenase
LPS	Lipopolysaccharide
MAO	Monoamine oxidases
MC	Myocardial cell
MCAO	Middle cerebral artery occlusion
MAPK	Mitogen activated protein kinase
MDA	Malonydialdehyde
MI	myocardial infarction
NF-κB	The Nuclear Factor κB
NO	Nitric oxide
Nrf2	The nuclear factor erythroid 2–related factor 2
OAT	m organic anion transporter
PLDGF	platelet-derived growth factor
PI3K	Phosphoinositide 3-kinase
PG	Prostaglandin

PGC-1α peroxisome proliferator-activated receptor-gamma coactivator-1α
PPAR   peroxisome proliferator-activated receptors
ROS   Reactive oxygen species
SIRT   Sirtuin
SMA   Smooth muscle actin
SOD   superoxide dismutase
TAK1   Transforming growth factor beta-activated kinase 1
TBARS   thiobarbituric acid reactive substances
TGF-β1   Transforming growth factor beta 1
Th   T helper
TLC   Thin layer chromatography
TLR   toll like receptor
TNF   Tumor necrosis factor
TXA   Thromboxane
UHPLC   ultra-high-performance liquid chromatography
URAT   m-urate anion transporter
VCAM-1   vascular cell adhesion molecules-1
VEC   vascular endothelial cells
VLC   Vacum liquid chromatography
VSMC   Vascular smooth muscle cells
WBC   White Blood Cell

Introduction

Stilbenoids are natural defense polyphenols that occur in many plant species. Resveratrol (3,5,4′-trihydroxy-*trans*-stilbene) is possibly the best-known polyphenolic phytoalexin, and has attracted extensive scientific attention due to its potential health benefits. It is prominently present in red wine, and believed to contribute to the so-called 'French paradox', where moderate consumption of wine is correlated with a low incidence of coronary heart disease. Polydatin (PLD, formal IUPAC name: (2*S*,3*R*,4*S*,5*S*,6*R*)-2-[3-hydroxy-5-[(*E*)-2-(4-hydroxyphenyl)ethenyl]phenoxy]-6-(hydroxymethyl)oxane-3,4,5-triol, also known as piceid, (*E*)-piceid, (*E*)-polydatin, *trans*-polydatin, 3, 5, 4'-trihydroxystilbene-3-*β*-glucopyranoside, *trans*-resveratrol-3-*O*-*β*-glucopyranoside) is a glucoside of resveratrol in which a glucose is transferred to the C-3 hydroxyl group (**Figure 1**). Two isomeric forms exist in nature, (*cis*- and *trans*-)-polydatin. *Cis*-resveratrol and *cis*-polydatin are typically found at lower concentrations and are often less biologically active than their *trans* forms (Ribeiro de Lima et al., 1999). We review the recent studies on *trans*-polydatin and refer to it as PLD in this review.

Resveratrol is well-known for its chemopreventive, antidiabetic, and neuroprotective properties (Rivière et al., 2012). However, recent studies highlighted that polydatin (PLD) may have higher bioavailability and possess better antioxidant activity than resveratrol (Wang et al., 2015). In addition, other bioactivities may be altered, e.g. whereas resveratrol inhibited tyrosinase with an IC_{50} value of 565 μM, PLD inhibited with an IC_{50} value of 14 μM, indicating that the glycosylation of resveratrol improved its tyrosinase inhibitory activity (Uesugi et al., 2017).
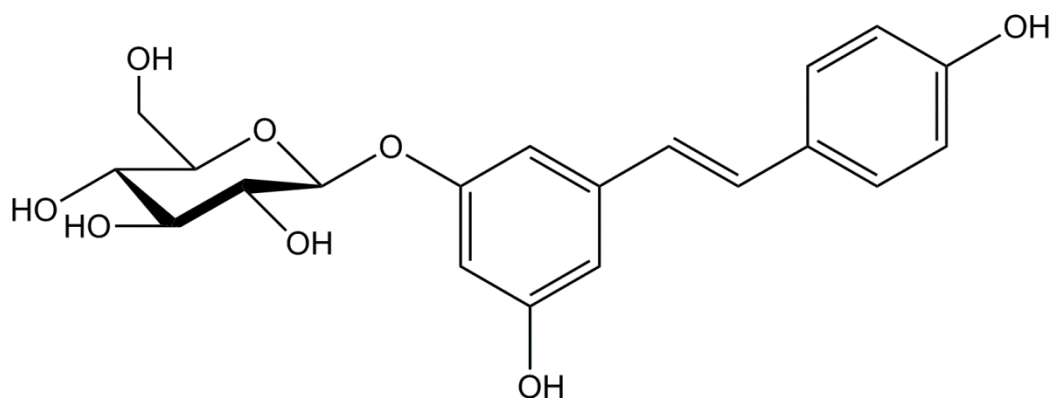
Figure 1. Structure of polydatin

PLD was first isolated from Japanese Knotweed (*Fallopia japonica*), but it also exists in a variety of other sources including dietary plants such as grape, peanut and berries. It is probably the most abundant form of resveratrol in nature. Glucose substitution gives PLD a more hydrophilic character than resveratrol and makes it more resistant to enzymatic oxidation. Further, the glucose groups make that PLD is more easily absorbed in the intestinal tract than resveratrol (Regev-Shoshani et al., 2003; Cao et al., 2016), resulting in a significantly increased bioavailability. The Chinese FDA has approved PLD for multiple phase II clinical trials mainly for anti-shock applications (Chen et al., 2015). It exhibits various biological activities such as anti-shock, anti-inflammatory, anti-oxidant, anti-cancer, anti-microbial, neuroprotective, lung protective and hepatoprotective effects (Du et al., 2013). In this paper, recent studies are reviewed on the natural occurrence of PLD, methods of analysis, biological effects, its bioavailability and metabolism, and the clinical studies conducted with this compound.

Natural sources

PLD was first reported in the peel of grapes. PLD is mainly present in red and white wines and grape juice; *cis*- PLD is the predominant form in rose and sparkling wines whereas *trans*-

Table 1. Natural sources of polydatin

Species	Parts	Family	References
Vateria indica L.	leaves	Dipterocarpaceae	Ito et al., 2012
Vatica rassak (Korth.) Blume	stem bark	Dipterocarpaceae	Tanaka et al., 2000
Upuna borneensis Symington	leaves	Dipterocarpaceae	Ito et al.,2017
Arachis hypogaea L.	seeds	Fabaceae	Ibern-Gómez et al., 2000
Lysidice brevicalyx C.F.Wei *L.rhodostegia* Hance	bark	Fabaceae	Hu et al., 2008
Erythrophleum lasianthum Corbishley	seeds	Fabaceae	Orsini et al., 1997
Quercus coccifera L.	stems, roots	Fagaceae	Sohretoglu et al., 2014
Iris tingitana Boiss. & Reut.	bulb	Iridaceae	Farag et al., 2009
Smilax glabra Roxb.	rhizome	Liliaceae	Zhang et al., 2016
Theobroma cacao L.	seeds	Malvaceae	Hurst et al., 2009
Morus atropurpurea Roxb.	fruit	Moraceae	Yang J et al., 2017
Abies koreana E.H.Wilson	leaf	Pinaceae	Jeon et al., 2015
Picea abies (L.) H. Karst., *P. jezoensis* (Siebold & Zucc.) Carrière	phloem root bark, stumps, needles	Pinaceae	Kiselev et al., 2016
Polygonum cuspidatum Siebold & Zucc.	roots, radix	Polygonaceae	Ma et al., 2013; Kimura et al. 1983
P. multiflorum Thunb, *P. reynoutria* Makino	roots	Polygonaceae	Feng et al., 2016
Rumex bucephalophorus L., *R. aquaticus* L.	roots, aerial parts	Polygonaceae	Orbán-Gyapai et al., 2017
Rheum australe D. Don	roots	Polygonaceae	Hu et al., 2014
Malus sp.	fruit	Rosaceae	Farneti et al., 2015
Rosa laevigata Tausch	roots	Rosaceae	Yan et al., 2014
Vitis vinifera L.	cell culture, seeds	Vitaceae	Sák et al, 2014
Parthenocissus tricuspidata (Siebold & Zucc.) Planch.	stems	Vitaceae	Jeon and Kim, 2013
Humulus lupulus L.	cone	Cannabaceae	Jerkovic and Collin, 2007; Jerkovic et al., 2008
Beeswax			Ares et al., 2015

resveratrol is more abundant in grapes, berries, peanuts and pistachios (Zamora-Ros et al., 2008). PLD can also be detected in many vegetable food and fruit, hop cones, hop pellets, beer, cocoa-containing products and chocolate products (Chiva-Blanch et al., 2011; Peng et al., 2015; Regev-Shoshani et al., 2003).

The predominant source of PLD are roots and rhizomes of *Fallopia japonica* (syn. *Polygonum cuspidatum* Siebold & Zucc., Polygonaceae), which have a long history of use in traditional Chinese (referred to as Huzhang) and Japanese Medicine (known as Itadori) as an analgesic, anti-pyretic, diuretic, anticancer and expectorant agent, and in the treatment of atherosclerosis (Jensen et al., 2010). However, the compound is present in several other genera like *Rosa, Rumex, Picea, Malus* and *Quercus* species (**Table 1**).

PLD has received similar attention to resveratrol because, in red wine and other grape products, the concentration of the glucoside usually exceeds that of the aglycone. The exact ratio of glycosylated to aglycone forms in wine depends on a number of factors such as method of fermentation and ecological conditions in the vineyards. Red wine contains up to 14.3 mg/l, and 29.2 mg/l of *trans*-resveratrol and PLD respectively, i.e. roughly equimolar amounts (60 - 70 µM) of the aglycone and glucosylated forms; white wines contain a factor 100 less (Galeano-Diaz et al., 2007). The higher concentrations in red wines are mostly due to the winemaking process: in the preparation of white wine, grapes are pressed and only the juice is fermented, whereas for red wine grape skins and seeds are removed only after the wine is fermented. On average, red grape skins are slightly richer in PLD and resveratrol than white ones, but differences between varieties or vintages of the same variety can be large (ranging from 50 - 200 mg/kg DW). Grape skins exhibit higher PLD contents than the seeds (Kammerer et al., 2004).

PLD was detected in 19 top selling commercially available cocoa-containing and chocolate products from the U.S. market. The cocoa-containing and chocolate products have about 3-5 times more PLD than free *trans*-resveratrol. Levels of PLD were highest in the cocoa powders (7.14 μg/g), followed by unsweetened baking chocolates (4.04 μg/g), semisweet chocolate baking chips (2.01 μg/g), dark chocolates (1.8 μg/g), milk chocolates (0.44 μg/g), and chocolate syrups (0.35 μg/g) (Hurst et al., 2009). Resveratrol and PLD contents in natural peanut butters were found to be significantly higher than those in blended peanut butter (Ibern-Gómez et al., 2000). Moreover, PLD was detected as the major stilbene derivative (4–8.8 mg/kg) in hop pellets (Jerkovic et al., 2005).

Biosynthesis, Biotransformation and Chemical Synthesis

Stilbenoids are synthesized via the phenylpropanoid and polyketide pathways. Resveratrol biosynthesis begins with the deamination of phenylalanine through phenylalanine ammonia lyase (PAL) to produce cinnamic acid, which is then hydroxylated by cinnamate-4-hydroxylase (C4H) to form *p*-coumaric acid. This product is attached to coenzyme A (CoA) via 4-coumarate-CoA ligase. Next, stilbene synthase (STS) condenses 4-coumaroyl-CoA with three molecules of malonyl-CoA to form the resveratrol (**Figure 2**), (Choi et al., 2014).

Subsequently, *trans*-resveratrol, may be further metabolized to form other stilbenoids, such as; polydatin via resveratrol glycosylation by glucosyltransferases (Kiselev et al., 2016).

PLD has also been generated on preparative scale through the microbial transformation of resveratrol by of *Bacillus cereus* strain UI 1477 (Cichewicz and Kouzi, 1998).

Cell suspension cultures of American pokeweed (*Phytolacca americana* L., Phytolaccaceae) could glucosylate *trans*-resveratrol to synthesize PLD (Ozaki et al., 2012).
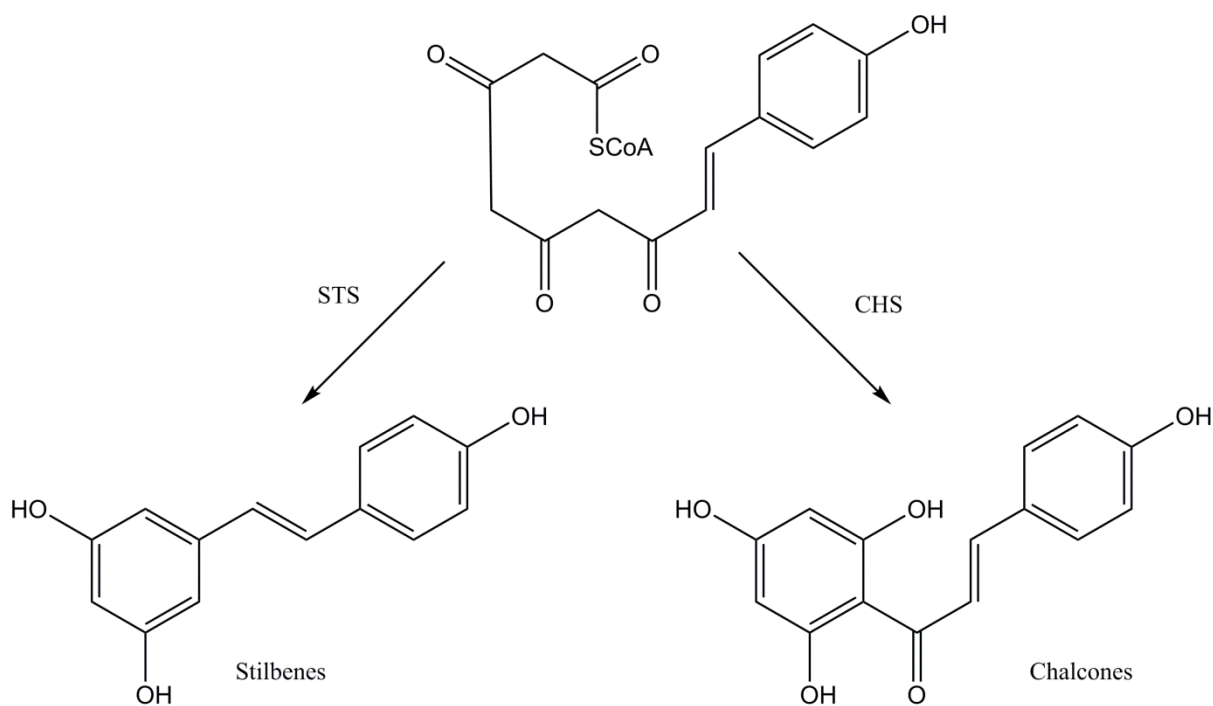
Figure 2. Resveratrol biosynthesis

A glucosyltransferase (GT) of *P. americana* (PaGT3) was expressed in *E. coli* and purified for use in the synthesis of two *O-β*-glucoside products of *trans*-resveratrol.

Resveratrol has been produced in engineered *Escherichia coli* expressing an artificial gene cluster that contains transgenes coding for tyrosine ammonia lyase, cinnamate/4-coumarate:coenzyme A ligase, caffeic acid *O*-methyltransferase, and stilbene synthase (Choi et al., 2011). Further addition of a UDP-glucosyltransferase transgene to the gene cluster resulted in *E. coli* that can produce PLD from simple carbon sources (Choi et al., 2014).

A range of resveratrol derivatives, including PLD, has been synthesized by means of Wittig reactions, followed by glucosylation under phase transfer catalysis (Orsini et al., 1997).

An alternative synthetic route to produce polydatin involves dropwise addition of *R*-bromotetra-*O*-acetyl-D-glucose (2.1 g, 5 mmol) in anhydrous MeOH (20 ml) to a stirred solution of NaOMe (230 mg, 10 mmol) and (*E*)-resveratrol (2.28 g, 10 mmol) in anhydrous MeOH (80 ml), at room temperature under argon atmosphere. The resulting solution was heated to 40 °C, under argon atmosphere, for 1 h. The dark brown solution was evaporated to dryness and the residue extracted with Et_2O. The suspension was filtered, and the filtrate evaporated to dryness. The crude residue was further purified by silica gel column chromatography, eluted with CH_2Cl_2/MeOH 8.5:1.5, to afford 170 mg of PLD (yield 25 %). The synthetic strategy proposed in this study represented an improvement over previously known procedures for PLD preparation, because large scale production of PLD is now achievable through a one-step reaction, starting from commercially available materials (Brandolini et al., 2002).

Extraction methods

Various used extraction methods to obtain PLD are given in **Table 2**.

Supercritical fluid extraction, with acetonitrile as modifier at 40 MPa, 100 °C has been used for the extraction of PLD from *F. japonica* and gave 0.22 mg/g yield (Beňová et al., 2010). Microwave-assisted extraction of resveratrol from the same plant species, using 1-butyl-3-methylimidazolium bromide solution has been reported to afford 2.65 mg/g yield of PLD (Du et al., 2007). Due to being simple, inexpensive and suitable for industrial purposes, ultrasound-assisted extraction has get more interest compared to other extraction methods.

Recently, multiple Response Surface Methodology and Box-Behnken designs were employed to investigate the affinities between the extraction variables (solvent concentration, extraction temperature and ultrasonic power) and response (extraction yield %), and to obtain the optimal conditions for extraction of PLD from *P. cuspidatum* (Kuo et al., 2014). Based on the

Table 2. Extraction methods of polydatin

Sample	Methods	Conditions	References
Polygonum cuspidatum Siebold & Zucc. (roots)	Solvent extraction Heated reflux extraction	60% aqueous ethanol 2 h reflux at 80 °C	Benova et al., 2008 Kuo et al., 2014
	Ultrasonic extraction Microwave- and ultramicrowave assisted extraction	room temperature, 1 h 10 min at 80 °C	Gao F et al., 2016
	Supercritical fluid extraction	acetonitrile	
Rheum australe D. Don (roots*)*	Solvent extraction	EtOH/H_2O (75:25), room temperature	Hu et al., 2014
Rosa laevigata Tausch (roots)	Solvent extraction under reflux	80% EtOH partitioned with petroleum ether, EtOAc and *n*-BuOH	Yan et al., 2014
Rumex bucephalophorus L. (roots and leaves)	Solvent extraction	acidified ethyl acetate (0.1% formic acid), room temperature	Kerem et al., 2006
R. aquaticus L. (aerial parts)	Percolation	MeOH, room temperature 50% aqueous MeOH partitioned with *n*-hexane, $CHCl_3$ and EtOAc	Orbán-Gyapai et al., 2017
Upuna borneensis Symington (leaves)	Solvent extraction	acetone	Ito et al., 2017
Vitis sp. (berry skins and leaves)	Solvent extraction	Methanol: ethyl acetate (50:50), 24h, 25 °C, darkness	Liu et al., 2013

model, and the consequent selection of appropriate extraction parameters, the extraction yields were improved. Under optimal conditions, the extraction yield of PLD from *P. cuspidatum* matched the predicted yield of 10.74 mg/g.

Isolation and Identification methods

The conventional methods of isolation PLD from crude plant extracts are based on liquid–liquid partition and silica gel column chromatography. These methods require a relatively long separation time, high consumption of organic solvents, and unsatisfactory resolution. There are various methods to obtain PLD from biological sources given in **Table 3.** Recently, high-speed counter-current chromatography (HSCCC) was used for fast and simple separation and high purification of PLD, and compared favourably to traditional column liquid chromatography (Bai et al., 2014; Chen et al., 2001; Chu et al., 2005).

A variety of analytical methods have been used to identify PLD. Organic solvent extraction, solid phase extraction, and direct injection techniques, have been used prior to resolution of resveratrol isomers by gas chromatography (GC) or high-performance liquid chromatography (HPLC). Most GC methods require derivatization with bis-[trimethylsilyl]-trifluoroacetamide (BSTFA) prior to injection into the GC, and are detected by flame ionization or mass-spectrometry (MS). Among the HPLC procedures, detection has been based upon UV-VIS, fluorescence, electrochemistry, chemiluminescence, diode array, MS, MS/MS (Cui et al., 2015; Glavnik et al., 2017; Soleas et al., 1997). Reversed phase columns, packed with n-octadecylsilane (ODS or C_{18}) bonded phase are commonly used for separation of PLD by HPLC. Details about the eluent systems, HPLC columns, and detection methods are summarized in **Table 4**.

Table 3. Different isolation methods of polydatin

Sample	Methods	Conditions	References
Abies koreana E.H.Wilson (leaves)	CPC DiaionHP resin C	ethyl acetate/isopropanol/water (9:1:10)	Jeon et al., 2015
Lysidice brevicalyx C.F.Wei (bark)	Polyamide CC Sephadex LH-20 ODS CC	H_2O:EtOH MeOH MeOH-H_2O (15:85-90:10)	Hu et al., 2008
Rheum australe D. Don (roots)	Si gel CC	Petroleum ether/acetone gradient $CHCl_3$/MeOH (90:10)	Hu et al., 2014
Rosa laevigata Tausch (roots)	Si gel CC	$CHCl_3$/MeOH (40:1-1:5) $CHCl_3$/MeOH (10:1-3:1)	Yan et al., 2014
R. aquaticus L. (aerial parts*)*	Si gel VLC Prep. TLC	$CHCl_3$/MeOH (99:1-1:1) CH_2Cl_2/MeOH (8:2)	Orbán-Gyapai et al., 2017
Upuna borneensis Symington (leaves)	RP CC Prep. TLC	MeOH/H_2O, MeOH, acetone, $CHCl_3$ EtOAc/$CHCl_3$/MeOH/H_2O (15:8:4:1)	Ito et al., 2017
Polygonum cuspidatum Siebold & Zucc.	HSCCC	chloroform/methanol/water (4:3:2). EtOAc/EtOH/H_2O (10:1:10, 70:1:10, 70:1:70) light petroleum/ethyl acetate/methanol/water (2:5:4:6), light petroleum/ethyl acetate/water (1:5:5)	Chen et al., 2001; Chu et al., 2005

Table 4. HPLC analysis of polydatin

Sample	Methods	Conditions	Detection	References
Rumex bucephalophorus L	RP HPLC	C18 (25x4.6 mm), 30 °C, flow rate 1 ml/min. A linear gradient using water and methanol, both acidified with 0.01% formic acid, following 2 min at 40% methanol and reaching 55% methanol in 8 min	DAD	Kerem et al., 2006
Lysidice brevicalyx C.F.Wei	RP HPLC	XDB-C18 (2.1 × 150 mm), 25 °C, flow rate, 0.8 mL/min MeOH:H2O gradient	DAD ESIMS	Hu et al., 2008
Red wine	normal phase HPLC	isocratic	DAD	Zhou et al., 2007; Gocan 2009
Polygonum cuspidatum Siebold & Zucc.	RP HPLC	LiChrospher C18, Ammonium acetate (pH 3) and ACN in gradient	multichannel CoulArray electrochemical detector 200–900 mV	Benova et al., 2008
Wine and grapes, Peanuts and Peanut Butter, *Polygonum cuspidatum* Siebold & Zucc.	RP HPLC	ODS Hypersil (250x4.6 mm), flow rate 1 ml/min 25% acetonitrile in 0.5% aqueous formic acid	DAD 307 nm fluorimeter operating 298 nm, 385nm	Burns et al., 2002
P. multiflorum Thunb	UHPLC	C18 (1.7 μm, 2.1×50 mm), flow rate 0.3 ml/min 0.1% formic acid aqueous solution (A) and acetonitrile (B) with a gradient	DAD	Chang et al., 2016
Foods	RP HPLC	Kromasil 100 C18 (150 mm x40 mm), flow rate 0.8 ml/min. water/acetonitrile/acetic acid (67:32:1) = B, acetonitrile = C, gradient, 0 min, 20% B; 18 min, 100% B; 28 min, 100% C; 33 min, 100% B and 37 min, 20% B.	DAD 280 nm Fluorometric	Moretón-Lamas et al., 2017

UV, MS, ^{1}H- and ^{13}C-NMR data which can be used to identify PLD are available through literature (Chu et al., 2005; Cichewicz and Kouzi, 1998; Jeon and Kim, 2013; Moreno-Labanda et al., 2004).

Biological properties

PLD shows no apparent toxicity; it did not reduce viability of human keratinocyte HaCaT cells up to 250 µM (He et al., 2012), and did not cause any cell death in primary hippocampal neuron cells up to 125 µM (Zhang Y et al., 2015). The acute toxicology of PLD was evaluated in mice by oral administration of 5000 mg/kg; no behavioral changes or deaths were observed over a period of 72 hours (Ni et al., 2017). However, the glucoside does have a wide range of potential therapeutic properties.

Figure 3. Biological properties of PLD

Anti-inflammatory effect

PLD modulates expression of some transcription factors and pro-inflammatory mediators both *in vivo* and *in vitro* in different test models. Anti-inflammatory action is one of the mechanisms underlying different beneficial effects of this compound.

In stimulated peripheral blood mononuclear cells, PLD inhibited Interleukin (IL)-17 production through downregulating of IL-17 mRNA expression in a dose dependent manner. At 20 µM, it inhibited IL-17 production 98 % whereas resveratrol caused 50% inhibition at this concentration (Lanzilli et al., 2012). In human epidermal keratinocytes (HaCat) that were induced with transforming growth factor-α (TGF-α), PLD at concentrations of 10-50 µM downregulated monocyte chemotactic protein-1 and interferon γ-produced protein of 10 kDa transcriptions, reduced tumor necrosis factor-α (TNFα), and IL-6 levels in normal human epidermal keratinocytes (HaCat) and significantly inhibited extracellular signal regulated kinase (ERK) and p65 phosphorylation (Pastore et al., 2012; Potapovich et al., 2011), but significantly enhanced IL-8 release.

Application of 44 µM PLD to heat-stressed HaCat cells, reduced IL-6, IL-8 and TNF- α levels, but upregulated toll like receptor (TLR)-2 expression. Simultaneously, it showed anti-inflammatory and cytoprotective effects by inducing the human β-defensin 2 and heat shock protein HSP70B′ expression (Ravagnan et al., 2013).

IL-1β (10 ng/ml) was used to induce apoptosis and ROS production in rat articular chondrocytes. Co-treatment with 20, 30 and 40 µg/ml PLD attenuated the IL-1β-induced processes, and increased chondrocyte viability. It led to reduced IL-1β-induced release of lactate dehydrogenase (LDH), superoxide dismutase (SOD), and NO levels, and it reduced the levels of TNF-α, IL-1β, IL-8 and COX-2. PLD decreased the levels of Bax, p-p38, and matrix metalloproteinase 13 and increased level of Bcl-2, while reducing the activity of caspase-3,

and the levels of pro-inflammatory cytokines (Yang G et al., 2017). From these experiments, it was concluded that PLD may protect against osteoarthritis, by acting on the p38 MAPK signaling pathway.

Histamine release from compound 48/80-induced rat peritoneal mast cells was inhibited by 29% after application of 1 μM PLD, and the effect was stronger than that of the aglycone resveratrol which inhibited by 15% (Shimoda et al., 2015).

Anti-inflammatory activity was also tested *in vivo*, using a variety of mouse or rat models where inflammation was artificially induced in a variety of ways, e.g. collagen‑induced arthritis (Li and Wang, 2016), D-galactose induced brain damage (Xu LQ et al., 2016), sepsis induced by puncture of the cecum (Zeng et al., 2015a), ligature-induced vascular damage (Gugliandolo et al., 2017), *Staphylococcus aureus*-induced mastitis (Jiang et al., 2017), surgically induced endometriosis (Di Paola et al., 2016), UVB-induced erythema in the epidermis of BALB ∕c-nu mice (He et al., 2012), or ov-albumin-induced hyperactivity in the small intestine of allergic rats (Yang et al., 2013). The *in vivo* experiments broadly confirm the *in vitro* assays: doses of 30 -100 mg/kg PLD decreased the artificially-induced over-expression of TLR2, and consequently inhibited TLR2-mediated activation of the p38 MAPK/NF-κB signaling pathway (Jiang et al., 2017). This in turn resulted in a decreased phosphorylation of NF-κB p65, and IκBα (Di Paola et al., 2016; Gugliandolo et al., 2017; Jiang et al., 2017; Zhao G et al., 2017), and attenuated a rise in TNFα, IL-1β, and IL-6 levels (Li and Wang, 2016; Xu LQ et al., 2016; Zeng et al., 2015a; Zhao G et al., 2017). PLD thus inhibited the iNOS production and generation of reactive oxygen species, apoptosis and activities of caspase 3 and 9 (Gugliandolo et al., 2017; Zeng et al.; Zhao G et al., 2017).

In mice with collagen induced-arthritis, 30 mg/kg PLD attenuated a rise in TNFα, and IL-6 levels; it was thought to act via activation of the expression of matrix metalloproteinase-9 (Li and Wang, 2016). It also attenuated D-galactose induced brain damage in mice by reducing TNF-α, IL-1β and IL-6 expression *in vivo* at 100 mg/kg (p.o) (Xu LQ et al., 2016).

45 mg/kg intravenous PLD also improved histopathological alterations in multiple-organ dysfunction syndrome induced by hemorrhage and ligation, and puncture of cecum-induced sepsis. It also reversed the increase in serum of advanced oxidative protein products, reduced TNF-α, IL-1β and IL-6 levels, and led to a decrease in Bax levels and caspase-3 activity and a concomitant increase in Bcl-2 levels in the kidney and liver in rats (Zeng et al., 2015a).

It inhibited nitric oxide (NO) and prostaglandin E2 (PGE2) production, and reduced inducible nitric oxide synthase (iNOS) and cyclooxygenase-2 (COX-2) expression at protein and transcriptional levels. It also inhibited lipopolysaccharide (LPS)-induced activation of ERK1/2, Jun N-terminal kinase (JNK), and p38 in Mouse monocyte macrophage (RAW) 264.7 cells. Inhibition of NO and PGE2 production is thought to be a result of the downregulation of phosphorylation of Nuclear Factor κB (NF-κB) and Mitogen-activated protein kinases (MAPK) (Lou et al., 2015). Also *in vivo*, in mice, PLD suppressed lipoteichoic acid-induced injury by attenuating ROS generation. PLD downregulated the lipoteichoic acid-induced NF-κB p65, and IκBα phosphorylation, resulting in a decrease in the transcription of TNF-α, IL-1β and IL-6. It thus inhibited the generation of reactive oxygen species (ROS), apoptosis and activities of caspase 3 and 9 (Zhao G et al., 2017).

PLD also protects from osteoarthritis, most likely by acting on the p38 MAPK signaling pathway. IL-1β (10 ng/ml) was used to induce apoptosis and ROS production in rat articular chondrocytes. Co-treatment with 20, 30 and 40 μg/ml PLD attenuated the IL-1β-induced processes, and increased chondrocyte viability. It led to reduced IL-1β-induced release of lactate dehydrogenase (LDH), superoxide dismutase (SOD), and NO levels, and it reduced the

levels of TNF-α, IL-1β, IL-8 and COX-2. PLD decreased the levels of Bax, p-p38, and matrix metalloproteinase 13 and increased level of Bcl-2, while reducing the activity of caspase-3, and the levels of pro-inflammatory cytokines (Yang G et al., 2017).

Experimentally induced vascular damage in mice was reduced by a palmitoylethanolamide: PLD (10:1) mixture, given by gavage at 30mg/kg. Treatment inhibited expression of intercellular and vascular adhesion molecules (ICAM-1 and VCAM-1), and suppressed inflammation by reducing pro-inflammatory factors TNF-α and IL-1β, iNOS production, and NFκB expression which in turn led to inhibition of Poly ADP-ribose polymerase formation, and inhibition of apoptosis via downregulation of Bax and Fas-ligand activation (Gugliandolo et al., 2017).

In mice with *Staphylococcus aureus*-induced mastitis, intraperitoneal administration of PLD at 15, 30, 45 mg/kg, down-regulated pro-inflammatory cytokine levels as TNF-α, IL-1β, IL-6 and IL-8, and decreased the expression of TNF receptor-associated factor-6, myeloid differentiation factor 88, IL-1 receptor-associated kinases (IRAK)-1 and IRAK4, and TLR2. Consequently, TLR2-mediated activation of the p38 MAPK/NF-κB signaling pathway was inhibited, which resulted in a decreased phosphorylation of Transforming growth factor β-activated kinase 1 (TAK1), MKK3/6, p38 MAPK, IκB-α and NF-κB (Jiang et al., 2017).

Treatment with palmitoylethanolamine: PLD 10 mg/kg (10:1) reduced the level and severity of the macroscopic and histological markers of experimentally induced endometriosis in rats. This treatment decreased angiogenesis, nerve growth factor, ICAM-1, matrix metalloproteinase 9 expression, and lymphocyte accumulation. It also reduced NFκB translocation and decreased the phosphorylation of Iκβa (Di Paola et al., 2016).

PLD suppressed UV-B induced expression of COX-2 and ROS production dose dependently by downregulating activation of p38, JNK and ERK1/2 in UVB-irradiated HaCaT cells, and 10 mg/kg treatment reduced UVB-induced erythema, desquamation, epidermal proliferation

and the expression of COX-2 and CD45 in the epidermis of BALB /c-nu mice (He et al., 2012).

PLD administration (orally, 150 mg/each) for 52 days after ov-albumin-induced hyperactivity in the small intestine of allergic rats, inhibited IgE production, secretion of Th2-type cytokine, IL-4, and decreased histamine levels in both serum and intestinal mucosa homogenates. It also decreased mast cell degranulation due to reduced $Ca^{2}+$ influx through store-operated calcium channels (Yang et al., 2013). 1 μM PLD inhibited histamine release from rat peritoneal mast cells by 29%, and its effect was stronger than that of the aglycone resveratrol which inhibited by 15% (Shimoda et al., 2015).

Anti-oxidant effect

Like other polyphenols, PLD exhibits high antioxidant activity through its ability to scavenge ROS and enhance the endogenous antioxidant defense system. It possesses significant antioxidant properties, due to its molecular structure of long-conjugated systems and polyphenol functions in the molecule. Studies have shown that PLD is more resistant to enzymatic oxidation than resveratrol. It seems that antioxidant mechanisms involving to most of biological effects of this compound. PLD scavenged DPPH (2,2-Diphenyl-1-(2,4,6-trinitrophenyl)-hydrazyl), ABTS (2,2'-Azino-*bis* (3-ethylbenzthiazoline-6-sulfonic acid) and •O_2^- radicals with IC_{50} values of 87, 20, 125 μg/ml, respectively *in vitro* (Xu LQ et al., 2016). Oxygen radical absorbance capacity values of PLD and resveratrol are 4.89 and 5.26 Trolox equivalents/μM respectively (Uesugi et al., 2017). PLD dose-dependently (0.05-2.00 mM) scavenges radical species and, in phenanthroline-Fe^{2+} system, possessed stronger hydroxyl radical scavenging capacity than resveratrol or vitamin C. Moreover, PLD dose-dependently (25-100 μM) protected human umbilical vein endothelial cells from H_2O_2 induced cell death (Su et al., 2013). PLD at 7.5 μM improved the cellular adhesion rate and enhanced the

migratory ability of human umbilical vein endothelial cells (HUVECs) injured by H_2O_2. At the same concentration, it also induced a remarkable decrease in the level of LDH by more than 50% and ROS by 18% and significantly attenuated the changes in the content of glutathione peroxidase (GSH-Px) by 33% and SOD by 60% compared to the H_2O_2 group Further, it reduced H_2O_2 induced apoptosis, decreased caspase-3 activity and proapoptotic protein Bax level, upregulated antiapoptotic protein Bcl-2 level. PD was concluded to suppress apoptosis in H_2O_2-injured HUVECs through inhibition of the protein kinase C signaling pathway. (Qiao et al., 2016). 240 μM PLD alone or in combination with 100 μM resveratrol synergistically suppressed oxidative stress by affecting the mitochondrial superoxide anions, extracellular NO production, and the antioxidant enzymes in Caco-2 cells, a colon cancer cell line (De Maria et al., 2013).

In mice and rats, oxidative stress was induced by single injection of 7 mg/kg cisplatin (Ince et al., 2014), weekly i.p. injections of 5-15 mg/kg doxorubicin (Wang et al., 2015),.chronic exposure to 100 mg/l arsenic through drinking water for 60 days (Ince et al., 2016), or daily subcutaneous injection with 200 mg/kg D-galactose for 8 weeks (Xu LQ et al., 2016). The markers used to determine the levels of oxidative stress are an increase in the level of malondialdehyde (MDA), and a concomitant decrease in activities of the enzymes superoxide dismutase (SOD), catalase (CAT), and glutathione peroxidase (GSH-Px); reduced GSH-Px activity results a decrease in glutathione (GSH) levels. Oral administration of PLD, at doses ranging from 25 - 100 mg/kg/day was shown to dose-dependently ameliorate or even reverse the damaging effects of oxidative stress injury (Ince et al., 2014, 2016; Wang et al., 2015; Xu et al., 2016),

Moreover, 50-200 mg/kg PLD treatment reduced the activity of several markers of tissue damage, i.e. aspartate aminotransferase (AST) (45 % lower at 200 mg/kg PLD), alanine aminotransferase (ALT) (33 % lower at 200 mg/kg PLD), in a dose dependent manner

compared to control (Xu LQ et al., 2016). Oral administration of PLD administration (50-100 mg/kg) for 8 weeks ameliorated D-Gal induced symptoms of aging, such as dullness, decreased activity, and shed hair in mice compared to control group (Xu LQ et al., 2016).

Anti-cancer effects

As for resveratrol, effects of PLD on tumour development have been investigated excessively using a variety of cell cultures and *in vivo* animal tumor models. An overview of the signaling pathways involved in the induction of cell death or inhibition of cell proliferation by PLD is given in **Figure 4**. Cytotoxicity of PLD for various cancer cell lines are given in **Table 5**.

PLD showed significant cytotoxicity at 50 μM and higher concentrations for HepG2, MCF-7 and MDA-MB-231 cells in a concentration- and time-dependent manner. It caused significant apoptosis in MDA-MB-231 cells at 100 μM and slight G1 cell cycle arrest (Su et al., 2013). PLD inhibited the proliferation of C2C12 mouse myoblast and PC3 human prostate cancer cell lines, and increased stress resistance via mechanism involving the Estrogen receptor β-mediated induction of Mn-superoxide dismutase in mitochondria (Robb and Stuart, 2014). 1–50 μM PLD showed concentration dependent growth inhibition on Caco-2 intestinal epithelial cell line through arresting the cell cycle in G0/G1 (10-25 μM) phase and inducing apoptosis. While 50 μM PLD treatment induced DNA fragmentation, resveratrol showed apoptosis at 100 μM concentration in Caco-2 cells (Storniolo et al., 2014). PLD inhibited the proliferation of RPMI 8226 multiple myeloma cells via mTOR/p70s6k signaling pathway. IC_{50} values of PLD are 131 μM and 93 μM in RPMI 8226 cells at 24 h and 48 h, respectively. PLD also induced apoptosis by downregulating Bcl-2 and increasing the caspase-3 and caspase-9, Bax levels in a dose-time dependent manner starting from 50 μM. It also induced autophagy by upregulating expressions of Beclin 1, Atg5 and LC3II at also same doses. It decreased the

Table 5. Cytotoxicity of polydatin on various cell lines

Cell line	Determining Method	IC$_{50}$ value (48h, μM)	References
RPMI 8226 Human Multiple Myeloma cells	Cell Counting Kit 8	93	Yang and Zhao, 2017
CCRF-CEM Human T Cell Leukemia	Resazurin reduction assay	25.08 ± 2.48	Kuete et al., 2015
CEM/ADR5000 Doxorubicin-Resistant Leukaemia Cells	Resazurin reduction assay	39.87 ± 2.91	Kuete et al., 2015
MDA-MB231 Human Breast Cancer Cells	Resazurin reduction assay	97.64 ± 7.60	Kuete et al., 2015
MDA-MB231/BCRP Human Breast Cancer Cells with Breast Cancer Resistance Protein	Resazurin reduction assay	95.59 ± 8.17	Kuete et al., 2015
HCT116 (p53+/+) p53 Resistance-Human Colon Carcinoma Cells	Resazurin reduction assay	63.77 ± 4.61	Kuete et al., 2015
HCT116 (p53−/−) Human Colon Carcinoma Cells	Resazurin reduction assay	47.03 ± 4.94	Kuete et al., 2015
U87MG Human Glioblastoma Cells	Resazurin reduction assay	55.64 ± 3.73	Kuete et al., 2015
U87MG.ΔEGFR Luciferase expressing Human Glioblastoma Cells	Resazurin reduction assay	47.59 ± 3.29	Kuete et al., 2015
AML12 Mouse Hepatocytes	Resazurin reduction assay	>102.56	Kuete et al., 2015
A549 Human Lung Adenocarcinoma Cells	MTT assay	2.95±0.37	Zhang et al., 2014
NCI-H1975 Non-Small Cell Lung Carcinoma Cells	MTT assay	3.23±0.46	Zhang et al., 2014
MDA-MB-231 Human Breast Adenocarcinoma Cells	MTT assay	2.66±0.73	Zhang et al., 2014
MCF-7 Human Breast Cancer Cells	MTT assay	1.49±0.26	Zhang et al., 2014
HeLa Human Cervical Cancer Cells	MTT assay	2.13±0.52	Zhang et al., 2014
SKOV-3 Human Ovarian Carcinoma Cells	MTT assay	4.44±0.89	Zhang et al., 2014
SMMC-7721 Human Hepatocarcinoma Cells	MTT assay	2.43±0.27	Zhang et al., 2014
CNE-1 Human Nasopharyngeal Carcinoma Cells	MTT assay	5.62±1.28	Zhang et al., 2014
HL-60 Human Promyeloctic Leukemia Cells	MTT assay	1.63±0.91	Zhang et al., 2014
K562 Human Leukemia Cells	MTT assay	1.91±0.37	Zhang et al., 2014

phosphorylation of mTOR and p70s6k compared with the control (Yang and Zhao, 2017).

PLD showed significant antiproliferative effects on different cancer cell lines (**Table 5**).

0-6 μM PLD decreased the Bcl-2 and cyclin D1 level in a lung cancer cell, but increased the

Bax level and induced S phase cell cycle arrest in a dose-dependent manner. Interestingly,

PLD showed less cytotoxicity on HBE non-cancerous human nasopharyngeal cell line.

(Zhang et al., 2014). 0-100 PLD μM dose-dependently induced apoptosis and inhibited the

proliferation of 143B and MG63 osteosarcoma cells and induced apoptosis by suppressing β-

catenin signaling and the increasing expression of Bax/Bcl-2 and caspase-3 activity (Xu G et

al., 2016). PLD showed antiproliferative effect and induced apoptosis in laryngeal cancer cell

Arrows represent activation, whereas bars represent inhibition
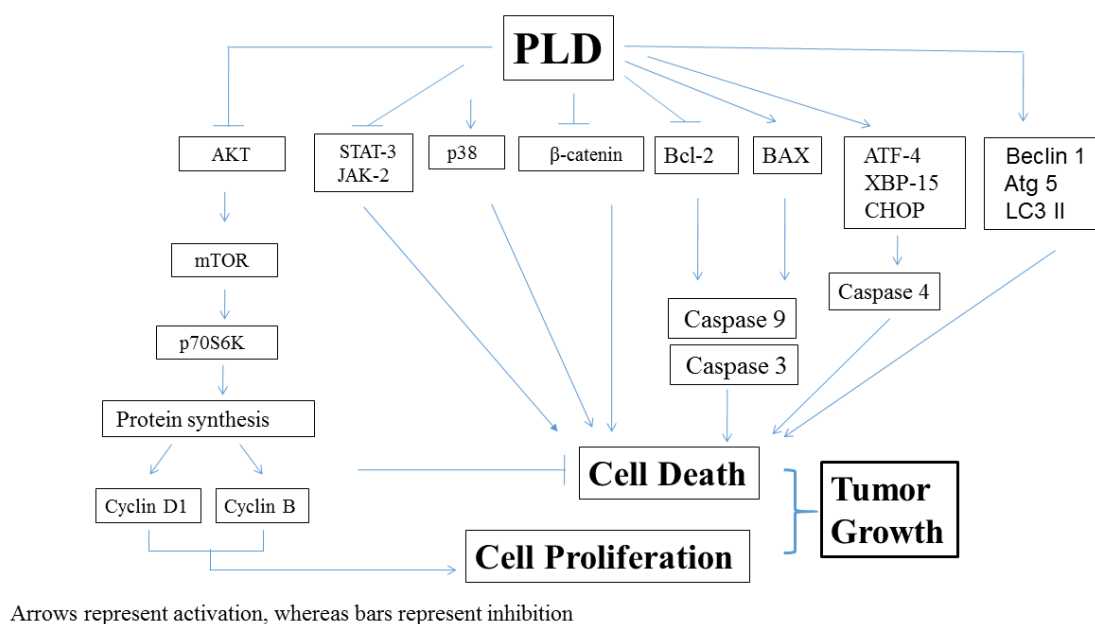
Figure 4. Signaling pathways involved in the induction of

cell death or inhibition of cell proliferation by PLD

lines (Hep-2 and AMC-HN-8), and HeLa cervix cancer cell line via platelet-derived growth

factor (PLDGF)/Akt pathway in time- and dose-dependent manner. It decreased PLDGF-B

and p-Akt levels without altering total Akt level. PLD affected cell differentiation and showed

cytotoxic effect on CaCo-2 human colon adenocarcinoma cells by reducing the expression of Hsp27 and vimentin (IC_{50} values are 72 and 192 μM for exponentially growing and post-confluent cells, respectively). 240 μM PLD treatment caused increase of the cleaved form of poly-(ADP-ribose) polymerase and G1 phase arrest. It also reduced total and phosphorylated forms of Akt. It upregulated p21 level and ERK1/2 phosphorylation in CaCo-2 cell line (De Maria et al., 2013). PLD reduced the growth of MDA-MB-231 and MCF-7 breast cancer cell lines by leading to cell S phase arrest in both cell lines. Molecular mechanism studies showed that it down-regulated the phosphorylation of Creb proteins and reduced the cyclin D1 expression dose dependently. It upregulated phosphorylation of Akt but the (Phosphoinositide 3-kinase) PI3K inhibitor wortmannin exhibited an insignificant effect on the cell survival, cell cycle, and apoptosis of PLD-treated breast cancer cells. Similarly, 2.5 μM PLD increased phosphorylations of p38 and ERK. However, cell growth inhibition, cell cycle arrest, and apoptosis induced by PLD were not affected by ERK inhibitor PLD98059 or p38 inhibitor SB203580. These results indicated that neither PI3K pathway nor MAPK pathway were involved in cell proliferation inhibitor effect of PLD (Chen et al., 2017). 0-20 μM PLD impeded the proliferation of MOLT-4 leukemia cells in a dose dependent manner. It induced apoptosis and blocked the cell cycle in S phase by increasing the Bcl-2/Bax ratio, and downregulated the cyclin B1 and D1 levels. It showed synergistic effect with Janus kinase 2 inhibitors, indicating JAK2‑STAT3 pathway is involved in PLD induced cell cycle arrest and apoptosis in MOLT-4 cell line (Cao et al., 2016). 0- 20 μM PLD induced apoptosis also in nasopharyngeal carcinoma cell line (CNE) through increasing the cytosolic cytochrome c, and decreasing the mitochondrial cytochrome c as compared with the drug-untreated group. It caused cleavage fragment of caspase-9 at 10 μM, but not cleavage fragment of caspase-8, suggesting that mitochondria-mediated intrinsic apoptosis pathway but not death receptor-mediated extrinsic apoptosis pathway might be involved in PLD-induced apoptosis.

Furthermore, PLD activated caspase-4, indicating of endoplasmic reticulum stress involved in PLD's effect on apoptosis. PLD induced endoplasmic reticulum stress by increasing ATF4, XBP-1S, and CHOP proteins (Liu et al., 2011). 30 μM PLD enhanced bone marrow stromal cells migration by activating of ERK 1/2, which can be beneficial for stem cell therapy (Chen et al., 2016).

In a tumor xenograft experiment using nude Male–female athymic BALB/c mice, PLD treatment (50mg/kg) led to a 40% decrease in tumor weight compared with the 0.9% saline-treated control group (Li H et al., 2017).

Anti-diabetic effect

Reduction of blood glucose level

PLD partly restored glucose and lipid metabolism in high fat and sugar-induced diabetic rats. Orally administered PLD, taken for 8 weeks at 75 mg/kg reduced the levels of fasting blood–glucose (from 26 mM down to 23 mM), glycosylated hemoglobin glucose or HbA1c (from 9% to 6%), glycosylated serum protein (from 2.1 mM to 1.2 mM), total cholesterol (from 3.6 mM to 1.4 mM), triglyceride (from 9.2 mM to 1.1 mM), and low-density lipoprotein cholesterol (from 1.6 mM to 0.2 mM) in diabetic rats. Furthermore, PLD markedly increased serum insulin levels in diabetic rats, and obviously activated the Akt signaling pathway in diabetic rat livers (Hao et al., 2014). PLD reduced altered lipid and glucose metabolisms in type 2 diabetes as well as 10 or 100 mg/kg PLD administered for 4 weeks (Wang et al., 2016).

Improvement in insulin action

Experiments done in vitro, with insulin-resistant HepG2 cells give an indication of the pathways that are involved in amelioration of type 2 diabetes. PLD regulated partly restored glucose and lipid metabolism in insulin resistant HepG2 cells. Furthermore, 20 μM PLD

significantly elevated glucose uptake and utilization, and diminished lipid accumulation in insulin resistant HepG2 cells. PLD markedly activated the Akt signaling pathway in insulin resistant HepG2 cells (Hao et al., 2014). At a concentration of 5 µM, PLD upregulated the protein levels of low density lipoprotein receptor and glucokinase by inhibiting proprotein convertase subtilisin/ kexin type 9 in insulin-resistant type HepG2 cells (Wang et al., 2016).

Amelioration of diabetes-induced secondary complications

Various further pathways are involved in the anti-diabetic effects of PLD. PLD reduces renal fibrosis and thus, inhibits diabetic nephropathy dose dependently. It reversed the advanced glycation-end products (AGE)-induced downregulation of Sirtuin 1 (Sirt1) at 10-20 µM. Further, it increased the nuclear content, antioxidant response element-binding activity, and transcriptional activity of the nuclear factor erythroid 2–related factor 2 (Nrf2) as well as Heme oxygenase 1 (HO-1) and SOD1 expression, leading to a reduction of ROS production. Thus, PLD decreased the expression of fibronectin (FN) and TGF-β1, and reduction of renal fibrosis mechanisms was explained by activation of Sirt1-Nrf2/ARE anti-oxidative pathway (Huang et al., 2015). 10- 30 µM PLD supplementation reactivated production of Casein kinase 2 interacting protein-1 (CKIP1) in diabetic mice. CKIP1 is another activator of the Nrf2/ARE anti-oxidative stress signaling pathway, again leading to a reduction of renal fibrosis in diabetic nephropathy (Gong et al., 2017).

Oral 100 mg/kg PLD administration for 8 weeks stabilized the mitochondrial morphology and attenuated mitochondrial malfunction in KKAy mice (mice with type 2 diabetes) (Ni et al., 2017). PLD at 25 mM attenuated mitochondrial malfunction in hyperglycemia-induced podocyte MPC5 cells that were cultured *in vitro*. It also reversed podocyte hyperglycemia-induced apoptosis by downregulating dynamin-related protein 1 (Ni et al., 2017).

High glucose level damages endothelial cells (EC), and impairs vascular endothelial cells (VECs)-mediated vasodilatation in isolated rat aorta rings that were mounted in organ chambers. PLD at 1, 3, 10 μM improved the histological damage to endothelial cells in rat thoracic aorta tissue. At the same doses, it significantly ameliorated the impaired relaxation response to acetylcholine in high glucose group, in a dose dependent manner, the maximal drug relaxation effect of acetylcholine % (E_{max}) increased by 2.1, 2.6, and 3.5 folds, respectively. It restored the relaxation under acetylcholine in high glucose group to that of normal glucose group the control and, restored endothelium-dependent relaxation. This effect is probably mediated through activation of the peroxisome proliferator-activated receptors (PPAR)-β signaling pathway, and acts by upregulating the expression of endothelial NO synthase (eNOS), enhancing eNOS activity, and downregulating the iNOS level, in turn resulting in increased release in the blood vessels of nitric oxide (NO, also known as endothelium-derived relaxing Factor - EDRF) . Thus, PLD effective to restored endothelial functions in high glucose conditions by PPARβ-NO signaling pathways (Wu Y et al., 2015).

Amelioration of renal injury and renoprotective effect

PLD reduced alterations in renal injury and also exhibited renoprotective effects in mice. PLD reduced hyperuremia by regulating ion transporter proteins. PLD given orally at 20 and 40 mg/kg significantly decreased serum uric acid, serum creatinine, and blood urea nitrogen (BUN) levels to their normal values, and increased clearance rate of urine creatinine and BUN to normal values in potassium oxonate-induced hyperuricemic mice. It showed antihyperuricemic and nephroprotective effects by regulating of expressions of some renal ion transporters, murine urate anion transporter (mURAT)1, mGLUT9, mAGCG2, murine
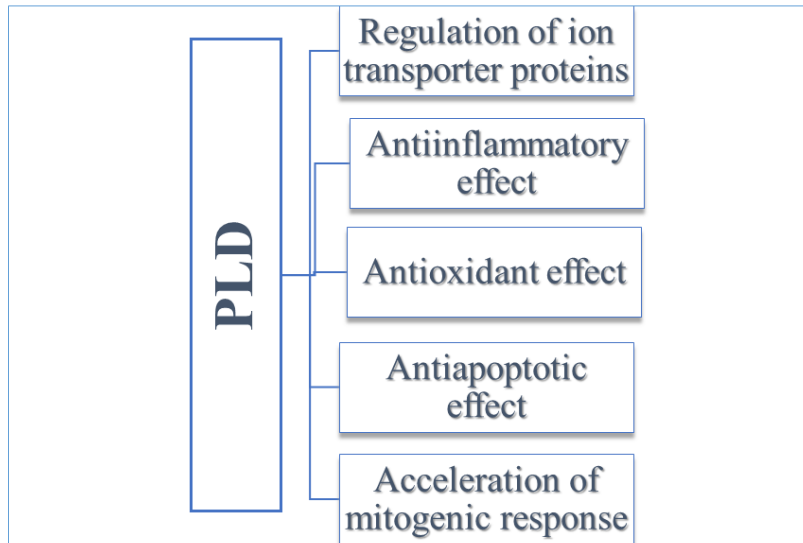
Figure 5. Mechanisms involved in amelioration

of renal injury and renoprotective effect of PLD

organic anion transporter (mOAT)1, mOCT1, mOCTN1, mOCTN2, and mUMOD, in hyperuricemic mice (Shi et al., 2012). 5, 10, 20 mg/kg PLD treatment for 7 days also reduced serum uric acid level through promoting uric acid excretion and regulating mURAT1, mOAT1 and mOAT3 (Wu et al., 2014).

Fructose-induced urate nephropathy in mice is marked by increased xanthine oxidase (XOD) activity. XOD catalyzes the oxidation of hypoxanthine to xanthine further to uric acid, in the process the enzyme generates reactive oxygen species. Oral PLD treatment at 25 mg/kg for 4 weeks decreased the serum urate level and reduced nephropathy effect by antioxidant and anti-inflammatory mechanisms in mice. It inhibited xanthine oxidase *in vitro*, with an IC_{50} value of 65.2 μM, which is 8 times less than the known XOD inhibitor allopurinol. However, this inhibition was competitive with Ki value of 47.2 μM. Moreover, treatment of fructose-induced nephropatic mice with 25 mg/kg PLD for 4 weeks enhanced the activity of SOD (going from 32.48 U/mg to 42.37 U/mg), GSH level (from 26 μg/g protein to,31.46 μg/g

protein), and reversed MDA level (from 26 nmol/mg protein to 20 nmol/mg protein). Oral administration of PLD at 25 - 50 mg/kg decreased expression of several markers of inflammation, i.e. NF-κB, p65, COX-2 and iNOS, and TNF-α, PGE2 and IL-1β. The anti-inflammatory effect of PLD was stronger than that of the XOD inhibitor allopurinol (Chen et al., 2013). PLD also showed antioxidative, anti-inflammatory, and nephroprotective effects in infusion /reperfusion (I/R) injury model through the PI3K/Akt pathway. It improved the renal function, accelerated the mitogenic response and reduced cell apoptosis in renal I/R models. Especially at 40 mg/kg intraperitoneal treatment, PLD significantly inhibited apoptosis in kidneys of mice after I/R, compared with vehicle control at 1 d, 3 d, 5 d, and 7 d after I/R *in vivo* and completely inhibited in HK-2 cells *in vitro*. 40mg/kg PLD strongly suppressed the renal I/R injury induced upregulation of the expression of THF-α, IL-1β, COX-2, iNOS, PGE-2, and NO levels after 3 days of renal I/R. PLD at 20 - 40 mg/kg also increased deteriorated activities of SOD, GST, GSH-Px and CAT, and the level of GSH. PLD dose-dependently upregulated the phosphorylation of Akt in I/R-injured mouse kidneys. It did not exhibit these effects when the PI3K/Akt pathway was inhibited (Liu et al., 2015). In continuation of this work, it was shown that 20 and 40 μM PLD exerted nephroprotective effects effecting cell apoptosis and oxidative stress against renal ischemia/reperfusion injury induced the secretion of sonic hedgehog (Shh), upregulated Ptch 1 and Smo - two key elements in Shh signaling, and enhanced the nuclear translocation and target gene transcription of Glioblastoma 1 (Gli-1) (Meng et al., 2016). PLD's protective effect in the renal I/R injury model also involves downregulation of I/R-induced expression of TLR4, and subsequent decreased expression of proinflammatory proteins NF-κB, TNF-α and IL-1β (Li Y et al., 2014). PLD suppressed high glucose-induced fibronectin production at 20 and 40 μM, it also inhibited NF-κB nuclear translocation, reduced the DNA-binding activity of NF-κB, and

decreased the protein expression of ICAM-1 and TGF-β in rat glomerular mesangial cells at 150 mg/kg (Xie et al., 2012).

Effects on the reproductive system

PLD exhibited protective effect against testicular torsion and detorsion injuries, at the histological, antioxidant stress and antiapoptotic levels. PLD treatment (intraperitoneal, 20 mg/kg) ameliorated the morphological damage, lowered the Cosentino histological score and increased the mean number of germ cell layers and Johnsen's testicular biopsy score in rats with testicular torsion and detorsion injury compared to control group. It reduced MDA level by 34.2% and enhanced CAT, GSH-Px and SOD activity by 53.0%, 66.0% and 26.7% respectively. It also decreased testicular torsion/detorsion induced germ cell-specific apoptosis 51.5 % by downregulating the activation of caspase-3, 8, and 9 and, poly(ADP-ribose) polymerase and upregulating the Bcl-2/Bax ratio (Qiao et al., 2017). PLD administration (oral, 200 mg/kg) almost completely prevented the arsenic-associated deterioration sperm morphology and reversed the arsenic-induced alteration of sperm motility (85.71 control, 58.57 arsenic, 71.42 50 mg/kg, 74.28 100 mg/kg PLD, 80.00 200 mg/kg PLD) and plasma membrane integrity. It reduced lipid peroxidation (MDA levels: 0.88 nmol/g control, 8.30 nmol/g arsenic, 4.52 nmol/g 50 mg/kg PLD, 2.09 nmol/g 100 mg/kg PLD, 1.25 nmol/g 200 mg/kg PLD) and increased antioxidant enzyme activities (SOD activities: 5.69 U/μg protein control, 2.43 U/μg protein arsenic, 3.45 U/μg protein 50 mg/kg PLD, 4.07 U/μg protein 100 mg/kg PLD, 4.38 U/μg protein 200 mg/kg PLD; CAT activities 44.65 k/ μg protein control, 15.52 k/μg protein arsenic, 15.16 k/μg protein 50 mg/kg PLD, 26.14 k/μg protein 100 mg/kg PLD, 31.92 k/μg protein 200 mg/kg) and regenerated tissue damage in testis of rats (Ince et al., 2016).

10 mg/kg/day palmitoylethanolamine: PLD (10:1) mixture was orally administered to rats with testosterone-induced benign hyperplasia for 14 days. This treatment decreased prostate weight and dihydrotestosterone production in testosterone-induced rats. It also reduced PGE2 and dihydrotestosterone levels, and downregulated expression of 5α reductase 1 and 5α reductase 2. This treatment also inhibited NF-κB translocation, and IκBα degradation reduced NOS and COX-2 levels, improved Nrf-2, HO-1 and Mn-SOD expressions, and decreased MDA level compared to control (Cordaro et al., 2017).

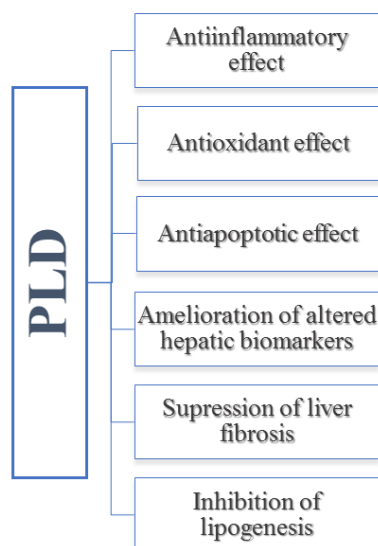**Hepatoprotective effect**

Figure 6. Mechanisms involved in amelioration of hepatoprotective effect of PLD

PLD exhibited strong hepatoprotective effects which are closely linked with anti-inflammatory and anti-oxidant actions. Oral 50 or 100 mg/kg PLD pre-treatment for 8 days significantly alleviated the alcohol-induced (10 ml 50% ethanol/kg) hepatic injury in mice, by reducing the serum liver injury markers, ALT and AST and decreasing relative liver weight and morphological deteriorations. It also ameliorated deteriorations in the hepatic antioxidant

enzyme levels as in the levels of reduced GSH, GST, glutathione reductase (GR), CAT, SOD and hepatic thiobarbituric acid reactive substances (TBARS), nitrite and carbonyl content. When 50 mg/kg PLD was compared with 25 mg/kg silymarin, PLD restored changes in GSH, GTH levels and SOD, NQO1 activities at the similar level with silymarin. PLD, more than silymarin, led to increased CAT activity, and decreased carbonyl and nitrites. However, silymarin reduced TBARS level and enhanced activity of GR more than PLD. It also reduced alcohol-induced increase expression of HO-1; prevented the rise in matrix metalloproteinase 2 and 9 activities and attenuated the increase in the NF- κB (p65) (Koneru et al., 2017).

After artificially induced hepatic failure in mice (e.g. by lipopolysaccharide-galactosamine, or carbon tetrachloride), 10-100 mg/kg PLD treatment diminished histopathological injury in liver, reduced ALT, AST levels, and lowered mortality (20 % 10 mg/kg PLD) in a dose-dependent manner. Moreover, it suppressed LPS-induced TNF-α production, myeloperoxidase activity, ICAM-1 and endothelial cell adhesion molecule-l (ECAM-1) expression, caspase-3 activation, and transcription of NF-κB activity (Wu et al., 2012). Pretreatment with 25, 50 and 100 mg/kg oral PLD for 5 days made that the levels of ALT, AST, MDA, activities of the antioxidant enzymes SOD and CAT activities, and expressions of TNF- α, IL-1β, COX-2, iNOS and NF-κB returned back to normal levels, whereas it upregulated mRNA and protein expression levels of hepatic TGF-β1 (Zhang H et al., 2012). Compared to the untreated mice with induced hepatic failure, levels of 25 - 100 mg/kg oral PLD dose dependently reduced ALT AST levels by up to 3-fold . Treatment decreased MDA level up to 1.4 fold, and increased activities of SOD, CAT, and GPx 1.5- fold, and GST levels up to 1.8 fold, respectively. The same treatment protocol reduced mRNA expression of TNF-α: 1.4, 2.2 and 2.3 fold, IL-1β: 1.2, 2.4 and 2.3 fold, COX-2: 1.4, 1.7 and 2.6, iNOS: 1.1, 1.4 and 1.6 fold, respectively, compared to CCl_4. Furthermore, 5 mg/kg intraperitoneal PLD suppressed level of a macrophage activation marker, CD68, and hepatic mRNA levels of

some inflammatory genes, TNF-α and monocyte chemoattractant protein-1, were also markedly increased in CCl$_4$-induced mice. PLD suppressed hepatic 4-hydroxynonenal (4-HNE) production, a sign of lipid oxidation, and nicotinamide adenine dinucleotide phosphate oxidative-4 expression, an inducer of profibrotic genes. In addition, PLD suppressed liver fibrosis by inhibiting collagen deposition (Zhao X et al., 2017).

Ameliorative effect on hepatic steatosis

PLD treatment (orally, 30 and 90 mg/kg) decreased hepatic steatosis and reduced plasma and liver triglyceride, total cholesterol and free fatty acid levels in high-fat diet fed rats. Moreover, it decreased TNF-α and MDA levels in the liver. PLD also downregulated the expression of some genes involved in lipogenesis, sterol-regulatory element binding protein1c, fatty acid synthase and stearoyl-CoA desaturase 1. Thus, PLD's effect in hepatic steatosis might partly associated with reduced TNF-α expression, lipid peroxidation level and SREBP-1c-mediated lipogenesis (Zhang J et al., 2012). Furthermore, PLD reduced the fat tissue and accumulation of lipids in the liver (liver index: 3.12 control, 2.97 control+PLD, 5.04 high-fat, 3.68 high-fat+PLD groups; epididymal fat 1.43 control, 1.39 PLD, 2.25 high-fat, 1.78 high-fat+PLD groups) induced in high-fat diet fed rats. It also reduced insulin resistance, decreased high-fat supplementation induced insulin and leptin levels. PLD treatment was also rescued high‑fat diet decreased insulin receptor substrate 2 and phosphorylated‑Akt protein expression in the liver (Zhang Q et al., 2015).

Effects on Neurodegenerative diseases

PLD exerted neuroprotective effects and improved learning and memory deficits in different experimental models.

Effects on memory function

Oral administration of 12.5, 25, 50 mg/kg PLD for 30 days attenuated cognitive deficits compared to the control in a rat model of vascular dementia induced by chronic cerebral hypoperfusion. 50 mg/kg PLD exhibited this effects in the similar manner with 25 mg/kg *Ginkgo biloba* extract. It also ameliorated deterioration of MDA level and SOD and CAT activities (Li et al., 2012). PLD treatment (intraperitoneally, 10 mg/kg) for 10 days enhanced long-term learning and memory in rats with perinatal hypoxic-ischemic brain injury through upregulating the expression of hippocampal brain-derived neurotrophic factor (Sun et al., 2014). PLD (intragastrically, 12.5 and 50 µg/ml) reduced ethanol-induced cell death rate and CDK5 expression in primary hippocampal neuron culture. It also reversed the performance impairments in chronic ethanol treated rats in Morris water maze test, especially 50 mg/kg PLD completely turned escape latency to normal level and rescued chronic ethanol administration-induced CDK5 expression (Zhang Y et al., 2015). 25 and 50 mg/kg PLD treatment improved memory acquisition and retention in permanent bilateral common carotid artery occlusion induced vascular disease and focal multiple infarction using homologous blood emboli induced vascular dementia models in the water maze tests (Xiao K et al., 2015).

Prevention and protection against cerebral ischemic injury

PLD showed neuroprotective effect by inhibiting both oxidative stress and mitochondria‑dependent apoptosis in a middle cerebral artery occlusion (MCAO) experimental model. PLD injection (30 mg/kg) to caudal vein 10 min prior to I/R injury reduced modified neurological severity scores and infarct volume after 24 h following I/R injury, in the PLD treated group. PLD treatment, significantly increased intracellular ATP levels, and decreased mitochondrial apoptosis through upregulation of Bcl-2 and downregulation of Bax, compared to MCAO group. PLD also lowered MCAO induced

activation of caspase‑3 and caspase-9, and reduced MCAO induced-ROS production (Gao Y et al., 2016). PLD protected the brain from damage caused by permanent MCAO. 50 mg/kg intraperitoneal PLD reduced body asymmetry in a Longa's neurological abnormality scores (4.1 at 24 hours, 4.2 at 72 h in vehicle and 2.6 at 24 hours, 2.1 at 72 hours in PLD after MCAO) and promoted the functional recovery of rats compared to control group. It also reduced MCAO-induced brain edema (84.4 % in vehicle, 80.0 % in PLD after 24 hours; 85.1 % in vehicle, 78.1 % in PLD after 72 hours) and volume of infarcts (42.5 % in vehicle, 37.3 % in PLD after 24 hours; 42.9 % in vehicle, 36.3 % in PLD after 72 hours). It up-regulated the expression of Gli-1, Ptch-1, and SOD1, and downregulated expression of NF-κB. PLD promoted the expression of claudin-5, a protein involved in regulation of blood-brain barrier permeability (Ji et al., 2012).

Effects on the aetiology of Parkinson's disease

20-100 mg/kg orally administered PLD dose-dependently attenuated rotenone-induced Parkinson's disease type defects like catalepsy and motor coordination disorder in male Sprague Dawley rats. Particularly, 80 mg/kg PLD group performed significantly better than the positive control group treated with 10 mg/kg L-dopa. PLD rescued rotenone-induced changes in the levels of GSH, ATP, MDA and manganese SOD in the striatum. PLD also alleviated the effects of chemically induced Parkinson's disease in mice and rats. It reversed dopaminergic neurodegeneration in the substantia nigra pars compacta region. Furthermore, oral PLD treatment prevented or alleviated motor deficits, increased SOD activity, and reduced MDA levels (Chen et al., 2015).

Effects on the aetiology of Alzheimer's disease

Alzheimer disease is characterized by the accumulation and polymerization of amyloid-β ($A\beta$) peptides. PLD inhibited $A\beta_{25-35}$ fibril formation in vitro, with an EC_{50} value of 4.7 μM probably via dynamic interaction between the PLD and the $A\beta$ that could open the hydrophobic zipper and shift the reversible equilibrium ''random coil $\leftrightarrow\beta$-sheet'' to the disordered structure (Rivière et al., 2007; 2009). PLD dose-dependently inhibited $A\beta$ polymerization, 0.1 mg/ml PLD also reversed decreased expression of $\alpha3$ and $\alpha7$ nicotinic acetylcholine receptors, another prominent factor in the etiology of Alzheimer's disease, in $A\beta_{1-42}$-induced SH-SY5Y cells in vitro (Xiao H et al., 2015).

Other neuroprotective effects

PLD addition (30 and 120 μM) to cultured cerebral cortical neurons reduced oxygen-glucose deprivation induced cell body damage, swelling, and cellular debris in a dose dependent manner (Zhang Y et al., 2015). Neuroglobin has neuroprotective role in stroke and neurodegenerative diseases. PLD upregulated both mouse and human neuroglobin promoter activity and increased neuroglobin mRNA expression in primary neurons (Liu et al., 2016). Monoamine oxidases (MAO) are neurotransmitters, while MAO-A inhibitors are used as antidepressants, MAO-B inhibitors, are relevant tools in the therapy of Alzheimer's and Parkinson's diseases. MAO inhibitors are also important with regard to their neuroprotective effects. PLD inhibited MAO mixed type with IC_{50} value of 85 μM, MAO-A 87 μM, and MAO-B 96 μM (Wei et al., 2016).

Effects on Pulmonary System

PLD exerted beneficial actions on pulmonary system underlying mechanisms generally associated with its antioxidant and anti-inflammatory effect.

PLD (intraperitoneal injection, 15, 45, and 100mg/kg) ameliorated sepsis-induced lung injury in a dose dependent manner by decreasing the TNF-α and IL-6 production, lung COX-2, and reducing the expression of iNOS and NF-κB activity in septic mice. Additionally, PLD increased the levels and activity of the new target of septic lung injury, HO-1 and abolished the effects of ZnPP IX (40 mg/kg), a specific HO-1 inhibitor (Li et al., 2013).

Due to its anti-inflammatory and antioxidant capacity, PLD showed protective effect in thoracic radiotherapy caused injuries. In an *in vivo* double controlled study on female C57BL/6 mice, treatment with PLD (100mg/kg/day by intraperitoneal injection, from 3 days prior to irradiation to 4 weeks after irradiation), reduced hyperemia and edema in lung tissues, alleviated structural damages and collagen deposit after irradiation. It also inhibited radiation-induced epithelial-mesenchymal transition by reversing upregulation of the interstitial markers vimentin and α-smooth muscle actin (α-SMA), and increased downregulated E-cadherin levels. It also alleviated increased acute inflammation and late fibrosis through inhibiting TGF-β1-Smad3 signaling pathway. Further, PLD regulated the balance of Th1- and Th2-type cytokines in acute lung injury. In cell culture studies, treatment with PLD (200-600 μM concentration range) increased the expression of Sirt3 and promoted Nrf2 and PGC1α levels on human bronchial epithelial cell line (BEAS-2B) and these findings suggested that Sirt3 may be a new potential target for PLD (Cao et al., 2017).

PLD, prevented the lung function impairment caused by airborne particles in polluted air through decreasing the oxidative potential *in vitro* and reducing the level of oxidative damage *in vivo.* Treating PM2.5-exposed rats (an inhalation injury animal model) with PLD (50 mg/kg, oral) for 8 weeks resulted in a notable increase in tidal volume, expiratory volume and minute ventilation volume comparing with the control group. Furthermore, PLD showed anti-inflammatory effect by reducing alveolar wall thickening and downregulating lymphocyte, monocyte, neutrophil, eosinophil and basophil and white blood cells in bronchoalveolar

lavage fluid, and inflammation-related lipids and pro-inflammatory cytokines, such as TNF-α and IL-1β in lung tissue (Yan et al., 2017).

PLD demonstrated protective effect on acute lung injury by acting on the anti-inflammatory TLR4-MyD88-NF-κB pathway *in vivo* and *in vitro*. PLD (80 mg/kg, intraperitoneal) treatment on LPS-induced acute lung injury models resulted in decreased levels of lung edema, polymorphonuclear, neutrophil numbers, TNF-α, IL-6, IL-1β, and a reversed activation of the TLR4-MyD88-NF-κB signaling pathway. Besides, PLD treatment at 2, 4 and 8 μM concentrations reduced the inflammatory cytokines levels (IL-1β, IL-6, IL-8 and TNF-α) and downregulated the expressions of TLR4, MyD88, NF-κB in LPS stimulated human bronchial epithelial BEAS-2B cells (Jiang et al., 2015).

PLD relieved the effects of burn-induced lung injuries and LPS-induced acute lung injuries due to its anti-inflammatory and anti-apoptotic effects. PLD treatment (intravenously, 45 mg/kg) on burn-injured rats resulted in a decrease of lung polymorphonuclear activity and polymorphonuclear leukocytes in bronchoalveolar lavage fluid, and levels of proinflammatory factors as TNF-α, IL-1 and IL-6 and pulmonary microvascular hyperpermeability. Also PLD decreased the number of apoptotic cells, by inhibition of caspase-3 activity and Bax/Bcl-2 ratio (Li et al., 2014a; Li et al., 2014b)

50 nM PLD ameliorated mitochondrial biogenesis and function of human pulmonary arteriolar smooth muscle cells *in vitro* by increasing the levels of Sirt1, mitochondrial DNA content, mitochondrial transcription factor A and cellular ATP. This may present another mechanism through which PLD can attenuate the effects of ischemic pulmonary injury (Li P et al., 2017).

Effect on Cardiovascular system

PLD exhibited various beneficial effects including post-myocardial infarction protective, vascular smooth muscle dilation, inhibition of platelet aggregation and thrombosis, blood pressure lowering and atherosclerosis prevention cardiomyocyte protective effects.

Post-myocardial infarction protective effect

PLD reduced hypertrophy of cardiomyocytes and heart failure in different test models. Reduction of mitochondrial biogenesis and function, and deterioration through autophagy and apoptosis in cardiomyocytes are related with heart failure. PLD (7.5 mg/kg by intraperitoneal injection for 10 days) showed protective effect in post- myocardial infarction (MI) cardiomyocytes via Sirt3 activation. PLD relieved mitochondrial dysfunction by amplifying ATP level, citrate synthase activity and complexes I/II/III/IV/V activities. Also 10 μM PLD suppressed apoptosis and upregulated autophagy by increasing GFP-LC3 puncta, and reducing the protein aggresomes and p62 in cultured neonatal mouse ventricular myocytes subjected to hypoxia for 6 h to simulate MI injury (Zhang et al., 2017). PLD (intraperitoneally 7.5 mg/kg) showed protective effects on post-myocardial I/R injury. It increased autophagy by promoting the degradation of autolysosome and decreased apoptosis in post-MI C57BL/6 mice experiment model and cultured neonatal rat cardiomyocytes. PLD treatment minimized the MI in size and increased the left ventricular fractional shortening and ejection fraction. Administration of 10 μM PLD to neonatal rat cardiomyocytes reduced mitochondrial membrane potential and cellular ROS, which were contributed the cardioprotective activity (Ling et al., 2016). PLD (30 - 50 μM) increased the cell viability and reduced apoptosis in cardiomyocytes subjected to simulated IR. It also reduced the infarct size and increased the cardiac function in IR mice related to the renin–angiotensin system and RhoA kinase (ROCK) pathway. PLD significantly eliminated the simulated IR –induced angiotensin I–II enrichment

and inhibited the activity of angiotensin-converting enzyme. Moreover, it inhibited ROCK activity, especially the angiotensin I receptor-activated ROCK pathway (Ming et al., 2017).

Effect on the aetiology of atherosclerosis

PLD (23 μM) inhibited the formation of foam cells derived from peritoneal macrophages. Macrophage cholesterol accumulation-induced foam cell formation is one of the hallmarks of atherosclerosis, PLD increased cholesterol efflux from macrophage and decreased the uptake of oxidized LDL, resulting in the inhibition of cholesterol accumulation in macrophage. Its mechanism may be regulated by PPAR-γ pathway (Wu M et al., 2015). PLD (25 - 100 mg/kg/day, oral) reduced low-density lipoprotein cholesterol/ high-density lipoprotein cholesterol and total cholesterol / high-density lipoprotein cholesterol ratios compared with the values obtained from high-fat/cholesterol hamsters. Further, the treatment decreased levels of serum total cholesterol, triglyceride, and low-density lipoprotein cholesterol, and treatment with 50 and 100 mg/kg doses of PLD also reduced hepatic triglyceride concentrations in high-fat/cholesterol hamsters. (Du et al., 2009).

Antihypertensive effect

PLD (100 mg/kg/day, 200 mg/kg/day intragastric) decreased ventricular collagen content, hypertrophy of cardiomyocytes, and heart mass index in ventricular remodeling induced by isoproterenol in mice statistically significant compared to positive control, metoprolol (60 mg/kg/day intragastric). Also treatment with PLD (60 mg/kg/day, 120 mg/kg/day intragastric) significantly reduced angiotensin II, endothelin-1 in left ventricular tissue, and aldosterone and TNF-α concentrations in serum comparing with captopril (40 mg/kg/day intragastric compared to positive control) leading to reduced blood pressure in rats (Gao et al., 2010). PLD also caused vascular dilation and microcirculation promotion by reducing intracellular

Ca concentration, activating vascular K^+ ATP channel and enhancing vascular activity through promoting extra-cellular sodium ion influx to cause cell depolarization (Liu et al., 2012).

Other cardioprotective effects

PLD (20–75 μM) attenuated phenylephrine-induced hypertrophy in cultured neonatal rat ventricular myocytes, and in a pressure overload-induced hypertrophic mouse model. PLD treatment inhibited the development of cardiac hypertrophy in cultured neonatal rat ventricular myocytes by increasing the cell surface area and decrease atrial natriuretic peptide and β- major histocompatibility complex levels. Also PLD acted as a barrier against Ca^{2+} - calcineurin- nuclear factor of activated T-cells pathway while keeping the cardiac contractility intact (Ding et al., 2014). PLD application (30 - 50 μM) reduced phenylephrine-induced oxidative stress and withheld Rho Kinase (ROCK) activation in cardiomyocytes. PLD also showed a similar effect in transverse aortic constriction applied mice as it suppressed the increased ROCK activity and decreased hypertrophic response and improved cardiac function (Dong et al., 2015).

PLD (intravenously, 10 mg/kg) improved cardiac dysfunction by correcting sarcoplasmatic reticulum Ca^{2+} leak that, after burn-injury, was mediated by hyperactive cardiac ryanodine receptors (RyR2) in an adult Sprague–Dawley rat experimental model. PLD reinstated Ca^{2+} load and Ca^{2+} levels in the sarcoplasmic reticulum. PLD treatment increased free thiol levels in RyR2 and reduced ROS (Jiang et al., 2013). Doxorubicin causes cardiotoxicity in patients who undergo chemotherapy. In order to evaluate the cardioprotective effect of PLD as well as its combination with vitamin C, male Sprague-Dawley rats divided into 4 groups and treated with doxorubicin, doxorubicin+PLD, doxorubicin+vitamin C and doxorubicin+PLD+Vitamin C for six weeks. PLD exhibited cardioprotective effect, however, combination therapy with

PLD (gavage, 100 μg/kg) and vitamin C (100 μg/kg) exhibited the best recovering effects on arterial pressure, heart rate, interval of QRS, GSH-Px activity. Both treatment ameliorated antioxidant parameters by enhancing activities of GSH-Px and SOD. PLD alone or combination with vitamin C also increased the mRNA expression levels of AMPK-α2 and PPAR- α without statistical difference in between each other in rats. Consistent with these results, PLD and vitamin C might relieve the myocardial toxicity caused by doxorubicin treatment (Wang et al., 2017). PLD has potential cardioprotective effects against Ca^2+ mishandling related heart diseases. Treatment with 1,10 and 100 μM PLD caused down-regulation of L-type Ca^2+ channel activity and upregulation of ryanodine receptor activity on rat ventricular myocytes and thus moderate decrease in Ca^2+ transient. Moreover, it increased myofilament Ca^2+ sensitivity in turn, increased myocyte contractility. It also modulated β-adrenergic receptor regulation of excitation–contraction coupling by alleviating β-adrenergic receptor stimulation-induced enhancement of Ca^2+ signaling without inhibiting β-adrenergic receptor mediated inotropic effect (Deng et al., 2012).

50 μM PLD inhibited the TNF-α stimulated endothelial cell–monocyte adhesion. 50 μM PLD could reduce the mRNA transcription and the protein levels of Intercellular Adhesion Molecule 1 (ICAM-1) and VCAM-1 in human umbilical vein endothelial cell by inhibiting of NF-kB pathway (Deng et al., 2011).

Anti-shock

PLD exhibits anti-shock effect, and the use of PLD in shock treatment approved by Chinese FDA (Chen et al., 2015). Administration of PLD (30 mg/kg) and norepinephrine (10 μg/kg) to 120 min shock subjected rats ameliorated hemorrhagic shock induced mitochondrial swelling, decreased mitochondrial membrane potential, and reduced intracellular ATP levels. It also maintained lysosomal stability, reduced activation of K_{ATP} channels, arteriolar smooth muscle

cells hyperpolarization, and reduced vasoresponsiveness to norepinephrine (Wang et al., 2012).

120 minutes after hemorrhagic shock, PLD (intravenous, 30 mg/kg) increased SIRT1 protein expression and activity in the intestine homogenate of normal control rats and restored SIRT1 and peroxisome proliferator-activated receptor-gamma coactivator-1α (PGC-1α) activity in small intestine during severe shock. The increased SIRT1 activity lead to increased SOD2 activity; in turn, attenuated oxidative stress levels and reduced apoptosis. PLD possess beneficial effects through SIRT1-PGC-1α-SOD2 axis in hemorrhagic shock (Zeng et al., 2015b). It also alleviated mitochondrial dysfunction occurred after hemorrhagic shock in kidney cells via the SIRT1-p53 pathway (Zeng et al., 2016). PLD showed beneficial effects on the heart function and microcirculatory perfusion in shock by causing various effects on vascular smooth muscle cells (VSMC), myocardial cells (MC), endothelial cells (EC), and white blood cell (WBC). PLD suppressed the ICAM-1 expression in LPS-induced EC, attenuated the adherence of WBC-EC and increased the Ca^{2+} levels in MC. Also PLD activated K^{+} ATP and decreased the pH value and Ca^{2+} levels of VSMC in shock (Zhao et al., 2003).

Anti-microbial activity

PLD has shown weak to moderate anti-microbial activity against a range of micro-organisms. It inhibited growth of *Helicobacter pylori,* with an MIC of 12.5 µM which is in the same order of magnitude as resveratrol (6.25 µM) (Khalil et al., 2016). In addition, PLD exhibited antibacterial activity against *Enterococcus faecalis*, *Staphylococcus aureus*, *S. saprophyticus*, *S. epidermidis*, *Escherichia coli*, *Klebsiella pneumoniae*, and *Salmonella typhimurium* with MIC values of 100, 400, 200, 200, 50, 25, 400 µg/ml, respectively. It possessed antifungal

activity against *Candida albicans* and *Trichophyton rubrum* with MIC values of 50 and 90 µg/ml, respectively. However, it only possessed a good antimicrobial activity against Gram negative bacteria, not to Gram positive bacteria or fungi, compared to positive control gentamycin for bacteria and clotrimazole for fungi (Mbosso et al., 2015). PLD further exhibited antibacterial activity against *Bacillus subtilis, B. epidermidis, Proteus vulgaris, Pseudomonas aeruginosa, Shigella dysenteriae* with MIC values of 20, 16, 24, 24, and 23 µg/ml. The MIC values found for PLD were about twice as high as those of positive controls, streptomycin, gentamycin or ciprofloxacin (Dar et al., 2016).

PLD exhibited an anti-*Leishmania amazonensis* activity with an IC_{50} values of 95 µM for promastigotes 29 µM for intracellular amastigotes. However, positive control amphotericin B IC_{50} values were found to be 0.1 µM for promastigotes 8.8 nM for intracellular amastigotes in the same study, indicating that PLD was not effective against to this organism (Passos et al., 2015).
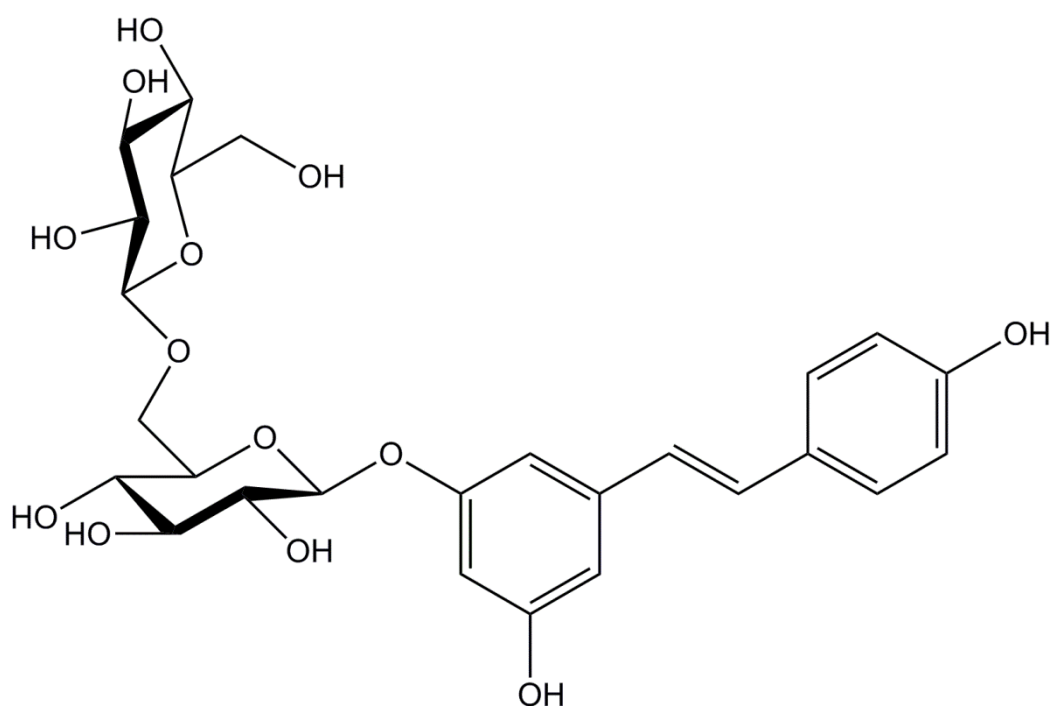

Figure 7. Structure of PLD-glucoside isolated from *Parthenocissus tricuspidata*

A PLD-related stilbenoid glycoside, PLD-(1→6)-β-D-glucopyranoside, isolated from *Parthenocissus tricuspidata* showed activity *in vitro* (IC_{50} 5.3 µM) and *in vivo* (orally, 5 mg/kg day) against *Plasmodium berghei* (**Figure 7**), (Son et al., 2007; Park et al., 2008).

Anti-osteoporotic activity

PLD administration (intraperitoneal, 10, 20 and 40 mg/kg/day) decreased body weight, and increased uterine index and dry weights of thigh-bones of ovariectomized mice compared to control. It increased the serum calcium, phosphorus, alkaline phosphatase and osteoprotegerin and of ovariectomized mice. It increased the serum calcium, phosphorus, alkaline phosphatase and osteoprotegerin and of ovariectomized mice. It upregulated the ratio of osteoprotegerin/ receptor activators of nuclear factor-κB ligand and β-catenin protein in ST2 (a bone marrow-stroma) cells. PLD possessed anti-osteoporotic activity via regulating osteoprotegerin, RANKL and β-catenin (Zhou et al., 2016).

Antithrombotic Effect

PLD concentration-dependently suppressed arachidonic acid-induced platelet aggregation *in vitro* and *in vivo*, and thus exhibited antithrombotic effect. The underlying activity mechanisms may be related to inhibition of platelet aggregation, which is related to a decrease of platelet cytosolic calcium and plasma thromboxane B2, and a concomitant increase in plasma 6-keto-$PGF_{1\alpha}$ level and suppression of platelet-neutrophil interactions (Chen et al., 2011).

Lifespan extension

1 mM PLD extended the mean lifespan of *Caenorhabditis elegans* by up to 30.7% and 62.1% under normal and acute stress conditions, respectively. The lifespan-extension role of PLD is associated to its anti-oxidative activity by regulating the aging-associated genes daf-16 and

stress-resistance protein SOD-3 involved in insulin/insulin like growth factor 1 signaling pathway (Wen et al., 2014).

Metabolism and pharmacokinetics of polydatin

The metabolism and pharmacokinetics of PLD follow a pattern common to most polyphenolic compounds. The absorption and metabolism in humans of the most abundant dietary polyphenols are well understood (Williamson & Clifford, 2017). Glycosides of polyphenolic compounds are generally believed to be hydrolyzed in the digestive tract, after which the aglycones are absorbed by the intestine epithelium and subsequently transported into the blood stream, where they are conjugated with glucuronic acid or sulphates as part of the phase II detoxification process.

Lactase (also known as lactase-phlorizin hydrolase, or LPH) is an enzyme that is active in the brush border of the small intestine epithelium. The enzyme is best known as the catalyst in the hydrolysis of the disaccharide lactose to form glucose and galactose, but it does accept a variety β-glucosides as substrates. LPH from rat small intestine cell-free extracts catalyzed hydrolysis of PLD, resulting in the formation of resveratrol and glucose (Henry-Vitrac et al., 2006). Caco-2 cultures growing on a polycarbonate membrane filter were used as an *in vitro* model for enterocytes lining the small intestine in a study on uptake, transport and metabolism of PLD (Henry et al., 2005; Henry-Vitrac et al., 2006). The picture that arises from the *in vitro* model studies is that PLD is partially hydrolyzed by LPH, after which resveratrol can passively diffuse into the lumen of the epithelial cells. Since intact PLD was also found inside the epithelial cells, a second, active transport mechanism is proposed involving sodium-dependent glucose transporter 1 (SGLT1), as had been reported previously for several other polyphenol glucosides (Walle and Walle, 2003; Hollman, 2004).

Transport of PLD or other glycosides of polyphenolic compounds across the membrane by SGLT1 is a matter of some controversy; the main argument in favor is that transport is reduced in the presence of either glucose or the SGLT1 inhibitor phlorizin. However, an alternative explanation for this observation is that glucose and phlorizin inhibit LPH and thus prevent hydrolysis of PLD or other glycosides, which results in a reduced amount of aglycones which constitute the main transport form (Kottra and Daniel, 2007). In this context, it may be worth noting that glucosides of polyphenolic compounds (including PLD) are efficiently hydrolyzed by LPH, more or less independent of the aglycone part of the glucoside. Other glycosides of polyphenolic compounds, e.g. galactosides, arabinosides, xylosides, rhamnosides, and galactosides, are poor substrates for LPH, and show much lower bioavailability than glucosides (Hollman, 2004). SGLT1 may still play a role in the kinetics of polyphenol uptake; recent results showed that, in addition to passive diffusion, SGLT1 in vascular endothelial cells actively transport free resveratrol (Chen et al., 2013).In humans, orally administered resveratrol is effectively absorbed in the ileum, but then rapidly converted into sulfate and glucuronic acid conjugates. Thus, the bioavailability of free resveratrol in circulating plasma is very low, although high accumulation may occur in epithelial cells along the digestive tract (Walle et al., 2004). It may be argued that, apart from in the digestive tract, free resveratrol levels will rarely be high enough to have any meaningful pharmacological effect. However, this assumes that resveratrol conjugates are biologically inactive, which may not be the case; the biological activity of PLD *in vitro* seems to exceed that of free resveratrol. Alternatively, PLD or other resveratrol conjugates may serve as an inactive precursor pool but are hydrolyzed to give resveratrol once they reach the target tissues (Santner et al., 1984; Walle et al., 2004).
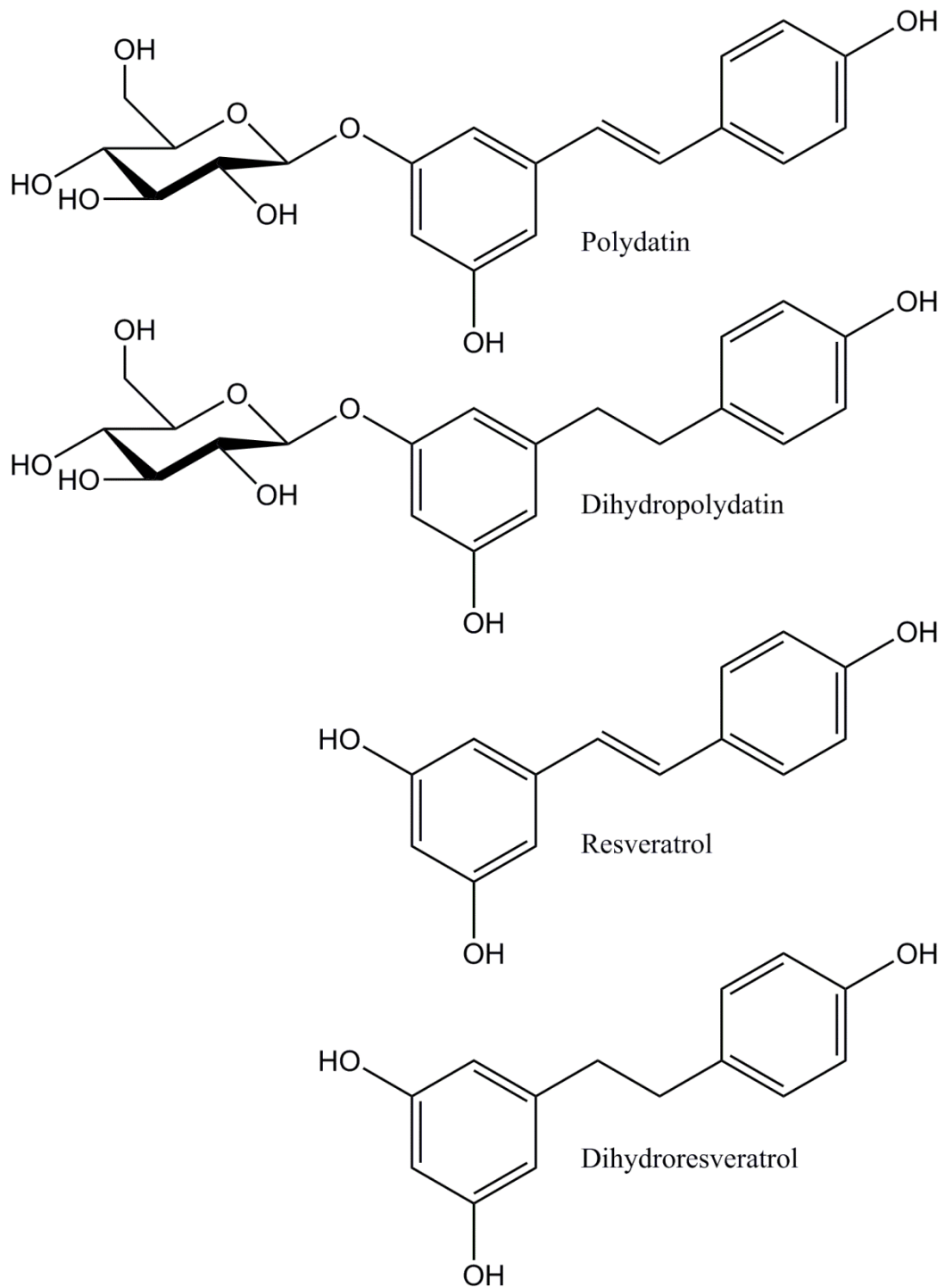
Figure 8. Fermentation products of PLD

Any PLD that is not hydrolyzed and/or absorbed in the ileum will be transported toward the colon where it is metabolized by the bacterial microflora. The metabolic steps typically

involve hydrolysis and dehydrogenation of the aglycone moiety. After the oral administration of *trans*-resveratrol to rats, dihydroresveratrol was the most abundant compound in urine and colon samples, followed by *trans*-resveratrol glucuronide- and sulfate-conjugates (Wang et al., 2005; Alfaras et al., 2010). Similar results were found in humans after oral consumption of red wine or grape extract tablets; dihydroresveratrol conjugates were the main metabolic products of resveratrol and PLD (**Figure 8**), (Rotches-Ribalta et al., 2012). An earlier attempt at profiling metabolic products of resveratrol failed to mention dihydroresveratrol conjugates (Burkon & Somoza, 2008), but this might be attributed to a lack of accurate analytical methods and absence of a commercially available pure standard at the time (Juan et al., 2010).

The high level of dihydroresveratrol conjugates as end metabolites after PLD consumption indicate that a substantial amount is not absorbed in the small intestine but passes unchanged into the large intestine. Several efforts have been made to increase the absorption of PLD.

PLD is poorly absorbed due to its large molecular size which prohibits passive diffusion, and is poorly lipid soluble. However, like other water soluble phytoconstituents, it can be bound to phospholipids, mostly phosphatidylcholine, resulting in a lipid compatible molecular complex, called a phytosome (Bhattacharya 2009). The molecular complex is held together by hydrogen bonds, and produces a little cell, whereby the plant extract is protected from destruction by gastric secretions owing to the gastroprotective property of phosphatidylcholine. A PLD phytosome was shown to double the oral bioavailability of polydatin in rats (Cheng et al., 2017).

Clinical trials

In a patient trial aimed at improving liver biochemical parameters, serum oxidative stress, and mental state, 20 chronic alcoholic patients that were hospitalized for rehabilitative therapy

were divided into two groups. A GSH and vitamin C (group 1), or a GSH, vitamin C and PLD (group 2) were treated for 2 weeks. GSH was administered twice a day (intravenously, 600 mg), 1 g vitamin C once per day (orally, 1 g), and 40 mg PLD twice a day (orally, 40 mg). Deteriorated ALT and AST levels were ameliorated compared to group 1, or to levels of these parameters at the beginning of treatment. Also, PLD treatment significantly reduced serum lipid peroxidation in alcoholic patients. Furthermore, Group 2 patient's cognitive functions improved, compared to beginning of treatment, whereas the recovery of the cognitive functions in group 1 at the end of treatment was not significant (Pace et al., 2015).

A pilot, 12-week, randomized, double-blind, placebo-controlled, multicenter study conducted on 54 irritable bowel syndrome (IBS) patients and 12 healthy volunteers to assess effect of palmithoylethanolamide/PLD 200 mg/20 mg. IBS patients showed higher mucosal mast cell counts (3.2 ± 1.3 vs. $5.3 \pm 2.7\%$, $p = 0.013$), reduced fatty acid amide oleoylethanolamide (12.7 ± 9.8 vs. 45.8 ± 55.6 pmol/mg, $p= 0.002$) and increased expression of cannabinoid receptor 2 (0.7 ± 0.1 vs. 1.0 ± 0.8, $p = 0.012$) compared with controls. The treatment did not significantly modify IBS biological profile, but compared to placebo, palmithoylethanolamide/PLD significantly improved abdominal pain severity ($p < 0.05$) (Cremon et al., 2017).

A pilot, 6 months, randomized, open-labeled, three arm study was conducted to evaluate the efficacy of treatment with palmithoylethanolamide/PLD on chronic pelvic pain related to endometriosis on thirty patients at reproductive age. Group A was administered palmithoylethanolamide 400 mg + PLD 40 mg 2 tablets daily for 6 months; group B leuprorelin acetate 11.25 mg, one vial every 3 months during 6 months, group C ethinylestradiol 0.03 mg + drospirenone 3 mg 1 tablet for 6 months were administered. This study showed that palmithoylethanolamide/PLD treatment was as effective as hormonal

therapy for reducing pain related to endometriosis without effecting ovulation (Di Francesco & Pizzigallo, 2014).

A randomized, placebo-controlled study on 220 women aged 16 to 24 years with primary dysmenorrhea conducted to evaluate the effectiveness of the association between palmitoylethanolamine and PLD on pelvic pain in primary dysmenorrhea. Patients treated with 400 mg + 40 mg palmitoylethanolamine + PLD combination (1 tablet a day for 10 days from the 24th day of cycle) or placebo (1 tablet a day for 10 days from the 24th day of cycle). An improvement of pelvic pain was seen in 98 % of cases in treatment group vs 56 % in placebo group (p < 0.001), indicated effectiveness of palmitoylethanolamine + PLD combination (Tartaglia et al., 2015).

A randomized, double-blind, placebo-controlled trial on twenty women with vestibulodynia received oral 400 mg + 40 mg palmitoylethanolamine + PLD combination or placebo, twice daily for 60 days to assess whether to see that palmitoylethanolamide + PLD combination may contribute to a down-regulation of mast cell hyperactivity, which is believed to be responsible for the proliferation and sprouting of vestibular pain fibers and the associated hyperalgesia and allodynia. This treatment improved symptoms especially in cases with more recent disease onset, as compared with the placebo group (Murina et al., 2013).

Conclusion

PLD, represents a new promising and well-tolerated therapeutic agent for the management of different pathologies, especially degenerative diseases. However, some biological activities that were reported are only seen *in vitro* at very high doses of PLD. The levels are considered unrealistic in *in vivo* experiments, and therefore not applicable to human use. Many studies explored metabolism of PLD or resveratrol in the body, showing that PLD is likely to convert into resveratrol (Wang et al., 2015), so, it could be regarded as a prodrug of resveratrol. It

seems that the mechanisms that underlie most of PLD's beneficial effects are related to cellular antioxidant and anti-inflammatory cascades. According to clinical trials, it seems a promising drug candidate especially for alleviation of chronic low-grade inflammation, and for pain management. Although PLD's bioavailability is higher than that of resveratrol, it remains a limiting factor in clinical applications, and novel formulations need to be designed to overcome this hurdle; liposome carriers and phytosomes have shown a good promise in this respect.

References

Alfaras I, Juan M E, Planas J M (2010) *trans*-Resveratrol reduces precancerous colonic lesions in dimethylhydrazine-treated rats. J. Agric. Food Chem. 58: 8104–8110. DOI: 10.1021/jf100702x

Ares A M, Gonzalez Y, Nozal MJ et al (2015) Development and validation of a liquid chromatography with mass spectrometry method to determine resveratrol and piceid isomers in beeswax J Sep Sci 38:197-204. DOI 10.1002/jssc.201400955

Bai B, Li C, Zhao Y et al (2014) One-step separation and purification of resveratrol and polydatin from *Polygonum cuspidatum* on 20% agarose beads J Liq Chromatogr Relat Technol 37:2733-2745. DOI 10.1080/10826076.2013.825864

Bhattacharya S (2009) Phytosomes: the new technology for enhancement of bioavailability of botanicals and nutraceuticals. International Journal of Health Research 2: 225-232. DOI: 10.4314/ijhr.v2i3.47905

Beňová B, Adam M, Onderkova K et al (2008) Analysis of selected stilbenes in *Polygonum cuspidatum* by HPLC coupled with coularray detection J Sep Sci 31:2404-2409. DOI 10.1002/jssc.200800119

Beňová, B.; Adam, M.; Pavlíková, P.; Fischer, J. (2010) Supercritical fluid extraction of piceid, resveratrol and emodin from Japanese knotweed. J. Supercrit. Fluids 51, 325–330.

Brandolini V, Maietti A, Tedeschi P et al (2002) Capillary electrophoresis determination, synthesis, and stability of resveratrol and related 3-O-β-D-glucopyranosides J Agric Food Chem 50:7407-7411

Burkon A, Somoza V (2008) Quantification of free and protein-bound trans-resveratrol metabolites and identification of trans-resveratrol-c/o-conjugated diglucuronides - two novel resveratrol metabolites in human plasma Mol Nutr Food Res 52:549-557. DOI 10.1002/mnfr.200700290

Burns J, Yokota T, Ashihara H et al (2002) Plant foods and herbal sources of resveratrol J Agric Food Chem 50:3337-3340

Cao K, Lei X, Liu H et al (2017) Polydatin alleviated radiation-induced lung injury through activation of sirt3 and inhibition of epithelial-mesenchymal transition J Cell Mol Med DOI 10.1111/jcmm.13230

Cao W J, Wu K, Wang C et al (2016) Polydatin-induced cell apoptosis and cell cycle arrest are potentiated by janus kinase 2 inhibition in leukemia cells Mol Med Rep 13:3297-3302. DOI 10.3892/mmr.2016.4909

Chang YX, Ge AH, Jiang Y et al (2016) A bioactivity-based method for screening, identification of lipase inhibitors, and clarifying the effects of processing time on lipase inhibitory activity of P*olygonum multiflorum* Evid Based Complement Alternat Med 2016:5965067. DOI 10.1155/2016/5965067

Chen L, Han Y, Yang F et al (2001) High-speed counter-current chromatography separation and purification of resveratrol and piceid from *Polygonum cuspidatum* J CHROMATOGR A 907:343-346

Chen L, Lan Z, Lin Q et al (2013) Polydatin ameliorates renal injury by attenuating oxidative stress-related inflammatory responses in fructose-induced urate nephropathic FOOD CHEM TOXICOL 52:28-35

Chen ML, Yi L, Jin X, Xie Q, Zhang T, Zhou X, Chang H, Fu YJ, Zhu JD, Zhang QY, Mi MT (2013) Absorption of resveratrol by vascular endothelial cells through passive diffusion and an SGLT1-mediated pathway. J. Nutr. Biochem. 24: 1823–1829 doi: 10.1016/j.jnutbio.2013.04.003

Chen P, Yun Y, He B et al (2011) Preventive effect of polydatin against thrombosis: And its mechanism Afr. J. Biotechnol 10:14177-14185

Chen S, Tao J, Zhong F et al (2017) Polydatin down-regulates the phosphorylation level of Creb and induces apoptosis in human breast cancer cell PloS one 12:e0176501. 10.1371/journal.pone.0176501

Chen Y, Zhang D, Liao Z et al (2015) Anti-oxidant polydatin (piceid) protects against substantia nigral motor degeneration in multiple rodent models of parkinson's disease Mol Neurodegener 10:4

Chen Z, Wei Q, Hong G et al (2016) Polydatin induces bone marrow stromal cells migration by activation of ERK1/2 Biomed Pharmacother 82:49-53. DOI 10.1016/j.biopha.2016.04.059

Cheng W, Li X, Zhang C et al (2017) Preparation and in vivo-in vitro evaluation of polydatin-phospholipid complex with improved dissolution and bioavailability Int J Drug Dev & Res 9:39-43

Chiva-Blanch G, Urpi-Sarda M, Rotches-Ribalta M et al (2011) Determination of resveratrol and piceid in beer matrices by solid-phase extraction and liquid chromatography-tandem mass spectrometry J Chromatogr A 1218:698-705. DOI 10.1016/j.chroma.2010.12.012

Choi O, Wu CZ, Kang SY, Ahn JS, Uhm TB, Hong YS (2011) Biosynthesis of plant-specific phenylpropanoids by construction of an artificial biosynthetic pathway in *Escherichia coli* J Ind Microbiol Biotechnol 38:1657–1665. DOI 10.1007/s10295-011-0954-3

Choi O, Lee J K, Kang SY et al (2014) Construction of artificial biosynthetic pathways for resveratrol glucoside derivatives J Microbiol Biotechnol 24:614-618

Chu X, Sun A, Liu R (2005) Preparative isolation and purification of five compounds from the chinese medicinal herb *Polygonum cuspidatum* sieb. Et zucc by high-speed counter-current chromatography J Chromatogr A 1097:33-39. DOI 10.1016/j.chroma.2005.08.008

Cichewicz R and HKouzi SA (1998) Biotransformation of resveratrol to piceid by *Bacillus cereus* J Nat Prod 61:1313-1314

Cordaro M, Impellizzeri D, Siracusa R et al (2017) Effects of a co-micronized composite containing palmitoylethanolamide and polydatin in an experimental model of benign prostatic hyperplasia Toxicol Appl Pharmacol 329:231-240. DOI 10.1016/j.taap.2017.06.005

Cremon C, Stanghellini V, Barbaro MR et al (2017) Randomised clinical trial: The analgesic properties of dietary supplementation with palmitoylethanolamide and polydatin in irritable bowel syndrome Aliment Pharmacol Ther 45:909-922. DOI 10.1111/apt.13958

Cui L, Wu Y, Han S (2015) Determination of polydatin by gold nanoparticle-enhanced chemiluminescence of silver nitrate and luminol Instrum Sci Technol 44:163-171. DOI 10.1080/10739149.2015.1081935

Dar BA, Lone SH, Shah WA et al (2016) LC-MS guided isolation of bioactive principles from *Iris hookeriana* and bioevaluation of isolates for antimicrobial and antioxidant activities Drug Res 66:427-431

De Maria S, Scognamiglio I, Lombardi A et al (2013) Polydatin, a natural precursor of resveratrol, induces cell cycle arrest and differentiation of human colorectal Caco-2 cell J Transl Med 11:264

Deng J, Liu W, Wang Y et al (2012) Polydatin modulates ca(2+) handling, excitation-contraction coupling and beta-adrenergic signaling in rat ventricular myocytes J Mol Cell Cardiol 53:646-656. DOI 10.1016/j.yjmcc.2012.08.009

Deng Y H, Alex D, Huang H Q et al (2011) Inhibition of TNF- α- mediated endothelial cell–monocyte cell adhesion and adhesion molecules expression by the resveratrol derivative, trans- 3, 5, 4′- trimethoxystilbene Phytother Res25:451-457

Di Paola R, Fusco R, Gugliandolo E et al (2016) Co-micronized palmitoylethanolamide/polydatin treatment causes endometriotic lesion regression in a rodent model of surgically induced endometriosis Front Pharmacol 7:382. DOI 10.3389/fphar.2016.00382

Ding W, Dong M, Deng J et al (2014) Polydatin attenuates cardiac hypertrophy through modulation of cardiac Ca 2+ handling and Calcineurin-NFAT signaling pathway Am J Physiol Heart Circ Physio307:H792-H802

Dong M, Ding W, Liao Y et al (2015) Polydatin prevents hypertrophy in phenylephrine induced neonatal mouse cardiomyocytes and pressure-overload mouse models Eur J Pharmacol 746:186-197

Du, F.Y.; Xiao, X.H.; Li, G.K. (2007) Application of ionic liquids in the microwave-assisted extraction of trans-resveratrol from *Rhizma Polygoni Cuspidati*. J. Chromatogr. A 1140, 56–62.

Du J, Sun LN, Xing WW et al (2009) Lipid-lowering effects of polydatin from *Polygonum cuspidatum* in hyperlipidemic hamsters Phytomedicine 16:652-658

Du QH, Peng C, Zhang H (2013) Polydatin: A review of pharmacology and pharmacokinetics Pharm Biol 51:1347-1354

Farag SF, Takaya Y, Niwa M (2009) Stilbene glucosides from the bulbs of iris tingitana Phytochem Lett 2:148-151. DOI 10.1016/j.phytol.2009.05.001

Farneti B, Masuero D, Costa F et al (2015) Is there room for improving the nutraceutical composition of apple? J Agric Food Chem 63:2750-2759. DOI 10.1021/acs.jafc.5b00291

Feng J, Ren H, Gou Q et al (2016) Comparative analysis of the major constituents in three related polygonaceous medicinal plants using pressurized liquid extraction and HPLC-ESI/MS Anal Methods 8:1557-1564. DOI 10.1039/c5ay02941d

Galeano-Diaz T, Duran-Meras, IAirado-Rodriguez D (2007) Isocratic chromatography of resveratrol and piceid after previous generation of fluorescent photoproducts: Wine analysis without sample preparation J Sep Sci 30:3110-3119. DOI 10.1002/jssc.200700285

Gao F, Zhou T, Hu Y et al (2016) Cyclodextrin-based ultrasonic-assisted microwave extraction and HPLC-PDA-ESI/MS separation and identification of hydrophilic and hydrophobic components of *Polygonum cuspidatum*: A green, rapid and effective process Ind Crops Prod 80:59-69. DOI 10.1016/j.indcrop.2015.10.039

Gao JP, Chen C X, Gu WL et al (2010) Effects of polydatin on attenuating ventricular remodeling in isoproterenol-induced mouse and pressure-overload rat models Fitoterapia 81:953-960

Gao Y, Chen T, Lei X et al (2016) Neuroprotective effects of polydatin against mitochondrial-dependent apoptosis in the rat cerebral cortex following ischemia/reperfusion injury Mol Med Rep 14:5481-5488. DOI 10.3892/mmr.2016.5936

Glavnik V, Vovk I, Albreht A (2017) High performance thin-layer chromatography–mass spectrometry of japanese knotweed flavan-3-ols and proanthocyanidins on silica gel plates J Chromatogr A 1482:97-108. DOI 10.1016/j.chroma.2016.12.059

Gocan S (2009) Analysis of stilbenes in wine by HPLC: Recent approaches J Liq Chromatogr Relat Technol32:1598-1643. DOI 10.1080/10826070902956352

Gong W, Li J, Chen Z et al (2017) Polydatin promotes nrf2-are anti-oxidative pathway through activating ckip-1 to resist hg-induced up-regulation of fn and icam-1 in gmcs and diabetic mice kidneys Free Radic Biol Med 106:393-405. DOI 10.1016/j.freeradbiomed.2017.03.003

Gugliandolo E, Fusco R, Biundo F et al (2017) Palmitoylethanolamide and polydatin combination reduces inflammation and oxidative stress in vascular injury Pharmacol Res 123:83-92. DOI 10.1016/j.phrs.2017.06.014

Hao J, Chen C, Huang K et al (2014) Polydatin improves glucose and lipid metabolism in experimental diabetes through activating the Akt signaling pathway Eur J Pharmacol 745:152-165. DOI 10.1016/j.ejphar.2014.09.047

He Y D, Liu YT, Lin QX et al (2012) Polydatin suppresses ultraviolet β-induced cyclooxygenase-2 expression in vitro and in vivo via reduced production of reactive oxygen species Br J Dermatol 167:941-944

Henry C, Vitrac X, Decendit A et al (2005). Cellular uptake and efflux of trans-piceid and its aglycone trans-resveratrol on the apical membrane of human intestinal Caco-2 cells J Agric Food Chem 53:798-803

Henry-Vitrac C, Desmoulière A, Girard D et al (2006) Transport, deglycosylation, and metabolism of trans-piceid by small intestinal epithelial cells Eur J Nutr 45:376-382

Hu L, Chen N, Feng L et al (2014) Piceatannol derivatives from *Rheum australia.* Don and their chemotaxonomic significance Biochem Syst Ecol. 55:369-373. DOI 10.1016/j.bse.2014.06.007

Hu Y, Ma S, Li J et al (2008) Targeted isolation and structure elucidation of stilbene glycosides from the bark of *Lysidice brevicalyx* guided by biological and chemical screening J Nat Prod 71:1800-1805

Hurst WJ, Glinski JA, Miller KB, Apgar J, Davey MH, Stuart SA (2008) Survey of the trans-Resveratrol and trans-Piceid Content of Cocoa-Containing and Chocolate Products J Agric Food Chem 56: 8374–8378

Ibern-Gómez M, Roig-Pérez S, Lamuela-Raventós R M et al (2000) Resveratrol and piceid levels in natural and blended peanut butters J Agric Food Chem 48:6352-6354

Ince S, Acaroz D A, Neuwirth O et al (2014) Protective effect of polydatin, a natural precursor of resveratrol, against cisplatin-induced toxicity in rats Food Chem Toxicol 72:147-153

Ince S, Avdatek F, Demirel H H et al (2016) Ameliorative effect of polydatin on oxidative stress- mediated testicular damage by chronic arsenic exposure in rats Andrologia 48:518-524

Ito T, Ito H, Oyama M et al (2012) Novel isolation of acetophenone derivatives with spiroketal-hexosefuranoside in upuna borneensis Phytochem Lett 5:325-328

Ito T, Ito H, Iinuma M (2017) Absolute configuration of resveratrol oligomer glucosides isolated from the leaves of *Upuna borneensis* Phytochem Lett 20:26-31. DOI 10.1016/j.phytol.2017.03.006

Jensen J S, Wertz C, FO'Neill VA (2010) Preformulation stability of trans-resveratrol and trans-resveratrol glucoside (piceid) J Agric Food Chem 58:1685-1690. DOI 10.1021/jf903009f

Jeon JS and Kim CY (2013) Preparative separation and purification of flavonoids and stilbenoids from parthenocissus tricuspidata stems by dual-mode centrifugal partition chromatography SEP PURIF TECHNOL 105:1-7. DOI 10.1016/j.seppur.2012.11.010

Jeon JS, Kim JH, Park CL et al (2015) Preparative isolation of polar antioxidant constituents from *Abies koreana* using centrifugal partition chromatography guided by DPPH•-HPLC experiment J Liq Chromatogr Relat Technol 38:1681-1686

Jerkovic V, Callemien D, Collin S et al (2005) Determination of stilbenes in hop pellets from different cultivars J Agric Food Chem 53:4202-4206

Jerkovic V, Collin S (2007) Occurrence of resveratrol and piceid in American and European hop cones J Agric Food Chem 55:8754-8758. DOI 10.1021/jf071792k

Jerkovic V, Nguyen F, Timmermans A et al (2008) Comparison of procedures for resveratrol analysis in beer: Assessment of stilbenoids stability through wort fermentation and beer aging J I BREWING 114:143-149. DOI 10.1002/j.2050-0416.2008.tb00319.x

Ji H, Zhang X, Du Y et al (2012) Polydatin modulates inflammation by decreasing nf-κb activation and oxidative stress by increasing Gli1, PTCH1, SOD1 expression and ameliorates blood–brain barrier permeability for its neuroprotective effect in PMCAO rat brain Brain Res Bull 87:50-59

Jiang K, Zhao G, Deng G et al (2017) Polydatin ameliorates staphylococcus aureus-induced mastitis in mice via inhibiting TLR2-mediated activation of the p38 MAPK/Nf-κb pathway Acta Pharmacol Sin 38:211

Jiang Q, Yi M, Guo Q et al (2015) Protective effects of polydatin on lipopolysaccharide-induced acute lung injury through TLR4-myd88- Nf-κb pathway Int Immunopharmacol 29:370-376. DOI 10.1016/j.intimp.2015.10.027

Jiang X, Liu W, Deng J et al (2013) Polydatin protects cardiac function against burn injury by inhibiting sarcoplasmic reticulum Ca2+ leak by reducing oxidative modification of ryanodine receptors Free Radic Biol Med 60:292-299. DOI10.1016/j.freeradbiomed.2013.02.030

Juan M E, Alfaras I, Planas J M (2010) Determination of dihydroresveratrol in rat plasma by HPLC. J. Agric. Food Chem. 58: 7472–7475 DOI:10.1021/jf100836j

Kammerer D, Claus A, Carle R et al (2004) Polyphenol screening of pomace from red and white grape varieties (*Vitis vinifera* L.) by HPLC-DAD-MS/MS J Agric Food Chem 52:4360-4367

Kerem Z, Bilkis I, Flaishman MA et al (2006) Antioxidant activity and inhibition of α-glucosidase by trans-resveratrol, piceid, and a novel trans-stilbene from the roots of Israeli *Rumex bucephalophorus* L J Agric Food Chem 54:1243-1247

Khalil AAK, Park WS, Kim HJ et al (2016) Anti-helicobacter pylori compounds from *Polygonum cuspidatum* Nat Prod Sci 22:220-224

Kiselev KV, Grigorchuk VP, Ogneva ZV et al (2016) Stilbene biosynthesis in the needles of spruce *Picea jezoensis* Phytochem 131:57-67. DOI 10.1016/j.phytochem.2016.08.011

Koneru M, Sahu B D, Gudem S et al (2017) Polydatin alleviates alcohol-induced acute liver injury in mice: Relevance of matrix metalloproteinases (MMPs) and hepatic antioxidants Phytomedicine 27:23-32. DOI 10.1016/j.phymed.2017.01.013

Kottra G, Daniel H (2007) Flavonoid glycosides are not transported by the human Na^+/glucose transporter when expressed in *Xenopus laevis* oocytes, but effectively inhibit electrogenic glucose uptake J. Pharmacol. Exp. Ther. 322:829–835 doi:10.1124/jpet.107.124040

Kuete V, Sandjo LP, Mbaveng AT et al (2015) Cytotoxicity of selected cameroonian medicinal plants and nauclea pobeguinii towards multi-factorial drug-resistant cancer cells BMC Complement Altern Med 15:309

Kuo C H, Chen B Y, Liu Y C et al (2014) Optimized ultrasound-assisted extraction of phenolic compounds from *Polygonum cuspidatum* Molecules 19:67-77. 10.3390/molecules19010067

Lanzilli G, Cottarelli A, Nicotera G et al (2012) Anti-inflammatory effect of resveratrol and polydatin by in vitro il-17 modulation Inflammation 35:240-248

Li B, Wang XL (2016) Effective treatment of polydatin weakens the symptoms of collagen-induced arthritis in mice through its anti-oxidative and anti-inflammatory effects and the activation of MMP-9 Mol Med Rep 14:5357-5362

Li H, Shi B, Li Y et al (2017) Polydatin inhibits cell proliferation and induces apoptosis in laryngeal cancer and hela cells via suppression of the PDGF/Akt signaling pathway J Biochem Mol Toxicol 31. DOI 10.1002/jbt.21900

Li P, Liu Y, Burns N et al (2017) Sirt1 is required for mitochondrial biogenesis reprogramming in hypoxic human pulmonary arteriolar smooth muscle cells Int J Mol Med 39:1127-1136. DOI 10.3892/ijmm.2017.2932

Li T, Cai S, Zeng Z et al (2014a) Protective effect of polydatin against burn-induced lung injury in rats Respir Care 59:1412-1421. DOI 10.4187/respcare.02831

Li T, Liu Y, Li G et al (2014b) Polydatin attenuates ipopolysaccharide-induced acute lung injury in rats : Int J Clin Exp Pathol 7:8401

Li X H, Gong X, Zhang L et al (2013) Protective effects of polydatin on septic lung injury in mice via upregulation of ho-1 Mediators Inflamm 2013:354087. DOI 10.1155/2013/354087

Li Y, Xiong W, Yang J et al (2014) Inhibitory effect of polydatin on expression of toll-like receptor 4 in ischemia-reperfusion injured nrk-52e cells Zhongguo Zhong yao za zhi= Zhongguo zhongyao zazhi= China journal of Chinese materia medica 39:3157-3161

Ling Y, Chen G, Deng Y et al (2016) Polydatin post-treatment alleviates myocardial ischaemia/reperfusion injury by promoting autophagic flux Clin Sci130:1641-1653

Liu H, Zhao S, Zhang Y et al (2011) Reactive oxygen species- mediated endoplasmic reticulum stress and mitochondrial dysfunction contribute to polydatin- induced apoptosis in human nasopharyngeal carcinoma cne cells J Cell Biochem112:3695-3703.

Liu LT, Guo G, Wu M et al (2012) The progress of the research on cardio-vascular effects and acting mechanism of polydatin Chin J Integr Med 18:714-719. 10.1007/s11655-012-1060-8

Liu CY, Wang LJ, Wang JF et al. (2013) Resveratrols in Vitis berry skins and leaves: their extraction and analysis by HPLC. Food Chem 136: 643–649.

Liu HB, Meng QH, Huang C et al (2015) Nephroprotective effects of polydatin against ischemia/reperfusion injury: A role for the PI3K/Akt signal pathway Oxid Med Cell Longev 2015:362158. DOI 10.1155/2015/362158

Liu N, Yu Z, Gao X et al (2016) Establishment of cell-based neuroglobin promoter reporter assay for neuroprotective compounds screening CNS Neurol Disord Drug Targets 15:629-639

Lou T, Jiang W, Xu D, Chen T, Fu Y (2015) Inhibitory Effects of Polydatin on Lipopolysaccharide-Stimulated RAW 264.7 Cells Inflammation 38: 1213-1220 DOI: 10.1007/s10753-014-0087-8

Ma P, Luo K, Peng Y et al (2013) Quality control of *Polygonum cuspidatum* by uplc-pda and related statistical analysis J Liq Chromatogr Relat Technol 36:2844-2854. DOI 10.1080/10826076.2012.723096

Mbosso JET, Kamdem LM, Jules C.A. Nguedia JCA et al (2015) In Vitro Evaluation of Antimicrobial and Antiproliferative Activities for Compounds Isolated from the *Ficus bubu* Warb. (Moraceae) Fruits: Chemotaxonomic Significance Drug Deliv Lett 5:122-131. DOI 10.2174/2210303105666151008213521

Meng Q H, Liu HB, Wang JB et al (2016) Polydatin ameliorates renal ischemia/reperfusion injury by decreasing apoptosis and oxidative stress through activating sonic hedgehog signaling pathway Food Chem Toxicol 96:215-225. DOI 10.1016/j.fct.2016.07.032

Ming D, Songyan L, Yawen C et al (2017) Trans-polydatin protects the mouse heart against ischemia/reperfusion injury via inhibition of the renin-angiotensin system (ras) and Rho kinase (ROCK) activity Food Funct 8:2309-2321. DOI 10.1039/c6fo01842d

Moreno-Labanda JF, Mallavia R, Pérez-Fons L et al (2004) Determination of piceid and resveratrol in spanish wines deriving from monastrell (*Vitis vinifera* L.) grape variety J Agric Food Chem 52:5396-5403

Moretón-Lamas E, Lago-Crespo M, Lage-Yusty MA et al (2017) Comparison of methods for analysis of resveratrol in dietary vegetable supplements Food Chem 224:219-223. DOI 10.1016/j.foodchem.2016.12.060

Murina F, Graziottin A, Felice R et al (2013) Vestibulodynia: Synergy between palmitoylethanolamide+ transpolydatin and transcutaneous electrical nerve stimulation Journal of lower genital tract disease 17:111-116

Ni Z, Tao L, Xiaohui X et al (2017) Polydatin impairs mitochondria fitness and ameliorates podocyte injury by suppressing DRP1 expression J Cell Physiol 232:2776-2787. DOI 10.1002/jcp.25943

Orban-Gyapai O, Liktor-Busa E, Kusz N et al (2017) Antibacterial screening of Rumex species native to the carpathian basin and bioactivity-guided isolation of compounds from *Rumex aquaticus* Fitoterapia 118:101-106. DOI 10.1016/j.fitote.2017.03.009

Orsini F, Pelizzoni F, Verotta L et al (1997) Isolation, synthesis, and antiplatelet aggregation activity of resveratrol 3-O-β-D-glucopyranoside and related compounds J Nat Prod 60:1082-1087

Ozaki S, Imai H, Iwakiri T et al (2012) Regioselective glucosidation of trans-resveratrol in *Escherichia coli* expressing glucosyltransferase from *Phytolacca americana* Biotechnol Lett 34:475-481. DOI 10.1007/s10529-011-0784-4

Pace M C, Passavanti M B, Aurilio C et al (2015) Polydatin administration improves serum biochemical parameters and oxidative stress markers during chronic alcoholism: A pilot study In Vivo 29:405-408.

Park W.H., Lee S.J., Moon H.I (2008) Antimalarial activity of a new stilbene glycoside from *Parthenocissus tricuspidata* in mice. Antimicrobial Agents and Chemotherapy 52: 3451–3453 DOI: 10.1128/AAC.00562-08

Passos C L A, Ferreira C, Soares D C et al (2015) Leishmanicidal effect of synthetic trans-resveratrol analogs PloS one 10:e0141778

Pastore S, Lulli D, Fidanza P et al (2012) Plant polyphenols regulate chemokine expression and tissue repair in human keratinocytes through interaction with cytoplasmic and nuclear components of epidermal growth factor receptor system Antioxid Redox Signal 16:314-328. DOI 10.1089/ars.2011.4053

Peng XL, Xu J, Sun XF et al (2015) Analysis of trans-resveratrol and trans-piceid in vegetable foods using high-performance liquid chromatography Int J Food Sci Nutr 66:729-735. DOI 10.3109/09637486.2015.1088934

Potapovich A I, Lulli D, Fidanza P et al (2011) Plant polyphenols differentially modulate inflammatory responses of human keratinocytes by interfering with activation of transcription factors Nfkb and AHR and EGFR-Erk pathway Toxicol Appl Pharmacol 255:138-149. DOI 10.1016/j.taap.2011.06.007

Qiao H, Chen H, Dong Y et al (2016) Polydatin attenuates H2O2-induced oxidative stress via pkc pathway Oxid Med Cell Longev 2016:5139458. DOI 10.1155/2016/5139458

Qiao H, Ma H, Cao W et al (2017) Protective effects of polydatin on experimental testicular torsion and detorsion injury in rats Reprod Fertil Dev. DOI 10.1071/RD17046.

Ravagnan G, De Filippis A, Carteni M et al (2013) Polydatin, a natural precursor of resveratrol, induces beta-defensin production and reduces inflammatory response Inflammation 36:26-34. DOI 10.1007/s10753-012-9516-8

Regev-Shoshani G, Shoseyov O, Bilkis I et al (2003) Glycosylation of resveratrol protects it from enzymic oxidation Biochemical Journal 374:157-163

Ribeiro de Lima M T, Waffo-Téguo P, Teissedre P L et al (1999) Determination of stilbenes (trans-astringin, cis-and trans-piceid, and cis-and trans-resveratrol) in portuguese wines J Agric Food Chem 47:2666-2670

Rivière C, Richard T, Quentin L et al (2007). Inhibitory activity of stilbenes on Alzheimer's β-amyloid fibrils in vitro. Bioorg Med Chem Lett 15:1160–1167

Rivière C, Delaunay JC, Immel F et al (2009). The polyphenol piceid destabilizes preformed amyloid fibrils and oligomers in vitro: Hypothesis on possible molecular mechanisms. Neurochem Res 34:1120–1128

Rivière C, Pawlus AD, Mérillon JM (2012) Natural stilbenoids: Distribution in the plant kingdom and chemotaxonomic interest in vitaceae Nat Prod Rep 29:1317-1333

Robb E L, Stuart J A (2014) The stilbenes resveratrol, pterostilbene and piceid affect growth and stress resistance in mammalian cells via a mechanism requiring estrogen receptor beta and the induction of Mn-superoxide dismutase Phytochem 98:164-173. DOI 10.1016/j.phytochem.2013.11.019

Rotches-Ribalta M, Andres-Lacueva C, Estruch R, Escribano E et al (2012) Pharmacokinetics of resveratrol metabolic profile in healthy humans after moderate consumption of red wine and grape extract tablets. Pharmacological Research 66: 375– 382 DOI: 10.1016/j.phrs.2012.08.001

Sák M, Dokupilová I, Mihálik D et al (2014) Elicitation phenolic compounds in cell culture of *Vitis vinifera* L. by *Phaeomoniella chlamydospora* Nova Biotechnologica et Chimica 13:162-171

Santner SJ, Feil PD, Santen RJ (1984) In situ estrogen production via estrone sulphatase pathway in breast tumours: relative importance versus aromatase pathway. J Clin Endocrinol Metab 59:29–33

Shi Y W, Wang C P, Liu L et al (2012) Antihyperuricemic and nephroprotective effects of resveratrol and its analogues in hyperuricemic mice Mol Nutr Food Res 56:1433-1444. DOI 10.1002/mnfr.201100828

Shimoda K, Kubota N, Uesugi D et al (2015) Synthesis and pharmacological evaluation of glycosides of resveratrol, pterostilbene, and piceatannol Ann N Y Acad Sci 1348:141-149

Soleas G J, Diamandis E P, Karumanchiri A et al (1997) A multiresidue derivatization gas chromatographic assay for fifteen phenolic constituents with mass selective detection Analytical Chemistry 69:4405-4409

Son, I.H., Chung, IM., Lee, SJ. et al. (2007) Antiplasmodial activity of novel stilbene derivatives isolated from *Parthenocissus tricuspidata* from South Korea. Parasitol Res 101: 237-241 DOI: 10.1007/s00436-006-0454-y

Storniolo C E, Quifer-Rada P, Lamuela-Raventos R M et al (2014) Piceid presents antiproliferative effects in intestinal epithelial caco-2 cells, effects unrelated to resveratrol release Food Funct 5:2137-2144. DOI 10.1039/c4fo00305e

Su D, Cheng Y, Liu M et al (2013) Comparision of piceid and resveratrol in antioxidation and antiproliferation activities in vitro PloS one 8:e54505. DOI 10.1371/journal.pone.0054505

Sun J, Qu Y, He H et al (2014) Protective effect of polydatin on learning and memory impairments in neonatal rats with hypoxicischemic brain injury by upregulating brainderived neurotrophic factor Mol Med Rep 10:3047-3051. DOI 10.3892/mmr.2014.2577

Sohretoglu D, Kuruuzum-Uz A, Simon A et al (2014) New Secondary Metabolites from *Quercus coccifera* L. Rec. Nat. Prod.8:323-329

Tanaka T, Ito T, Nakaya K et al (2000) Oligostilbenoids in stem bark of *Vatica rassak* Phytochem 54:63-69

Tartaglia E, Armentano M, Giugliano B et al (2015) Effectiveness of the association n-palmitoylethanolamine and transpolydatin in the treatment of primary dysmenorrhea J Pediatr Adolesc Gynecol 28:447-450. DOI 10.1016/j.jpag.2014.12.011

Uesugi D, Hamada H, Shimoda K et al (2017) Synthesis, oxygen radical absorbance capacity, and tyrosinase inhibitory activity of glycosides of resveratrol, pterostilbene, and pinostilbene Biosci Biotechnol Biochem 81:226-230. DOI 10.1080/09168451.2016.1240606

Walle T, Walle UK (2003) The β-D-glucoside and sodium-dependent glucose transporter 1 (SGLT1)-inhibitor phloridzin is transported by both SGLT1 and multidrug resistance-associated proteins. Drug Metabolism and Disposition 31: 1288–1291

Walle T, Hsieh F, DeLegge MH et al (2004) High absorption but very low bioavailability of oral resveratrol in humans. Drug Metab Dispos 32:1377–1382. DOI:10.1124/dmd.104.000885

Wang D, Hang T, Wu C et al (2005). Identification of the major metabolites of resveratrol in rat urine by HPLC-MS/MS J Chromatogr B, 829:97-106

Wang HL, Gao JP, Han YL et al (2015) Comparative studies of polydatin and resveratrol on mutual transformation and antioxidative effect in vivo Phytomedicine 22:553-559. DOI 10.1016/j.phymed.2015.03.014

Wang HL, Cui XH, Yu HL et al (2017) Synergistic effects of polydatin and vitamin C in inhibiting cardiotoxicity induced by doxorubicin in rats Fundam Clin Pharmacol 31:280-291

Wang X, Song R, Bian HN et al (2012) Polydatin, a natural polyphenol, protects arterial smooth muscle cells against mitochondrial dysfunction and lysosomal destabilization following hemorrhagic shock Am J Physiol Regul Integr Comp Physiol 302:R805-814. DOI 10.1152/ajpregu.00350.2011

Wang X, Guan Z-Z, Xiao-yan Hao X-Y (2015) Membrane permeability-guided identification of neuroprotective components from *Polygonum cuspidatum* Pharm Biol 52:3, 356-361

Wang Y, Ye J, Li J et al (2016) Polydatin ameliorates lipid and glucose metabolism in type 2 diabetes mellitus by downregulating proprotein convertase subtilisin/kexin type 9 (pcsk9) : Cardiovasc Diabetol 15:19

Wei B, Yang Z-D, Shi D-F et al (2016) Inhibition of monoamine oxidase by stilbenes from *Rheum palmatum* Iran J Pharm Res 15:885

Wen H, Gao X, Qin J (2014) Probing the anti-aging role of polydatin in *Caenorhabditis elegans* on a chip Integr Biol 6:35-43.

Wu G, Wu HJiang H (2014) Anti-hyperuricemia effect and mechanism of polydatin in mice Acta Pharm Sin 49:1739-1742

Wu M, Gong X, Jiang R et al (2012) Polydatin protects against lipopolysaccharide-induced fulminant hepatic failure in D-galactosamine-sensitized mice Int J Immunopathol Pharmacol. 25:923-934

Wu M, Liu M, Guo G et al (2015) Polydatin inhibits formation of macrophage-derived foam cells J Evid Based Complementary Altern Med. DOI 10.1155/2015/729017.

Wu Y, Xue L, Du W et al (2015) Polydatin restores endothelium-dependent relaxation in rat aorta rings impaired by high glucose: A novel insight into the PPARβ-NO signaling pathway PloS one 10:e0126249. 10.1371/journal.pone.0126249

Xiao H, Qi X-L, Liang Y, Lin C-Y et al. (2013) Membrane permeability-guided identification of neuroprotective components from *Polygonum cuspidatun*. Pharmaceutical Biology 52: 356-361, DOI: 10.3109/13880209.2013.837078

Xiao K, Li R, Sun M, Hou X et al (2015). Polydatin Use in Vascular Dementia. In: Martin CR, Preedy VR (ed) Diet and Nutrition in Dementia and Cognitive Decline Elsevier, London

Xie X, Peng J, Huang K, Huang J, Shen X, Liu P, Huang H (2012) PLD ameliorates experimental diabetes-induced fibronectin through inhibiting the activation of NF-κB signaling pathway in rat glomerular mesangial cells Mol. Cell Endocrinol 362: 183–193

Xu G, Kuang G, Jiang W et al (2016) Polydatin promotes apoptosis through upregulation the ratio of Bax/Bcl-2 and inhibits proliferation by attenuating the β-catenin signaling in human osteosarcoma cells Am J Transl Res. 8:922

Xu LQ, Xie YL, Gui SH et al (2016) Polydatin attenuates D-galactose-induced liver and brain damage through its anti-oxidative, anti-inflammatory and anti-apoptotic effects in mice Food Funct 7:4545-4555

Yan G, Li S, Hu J et al (2014) Phenolic constituents from the roots of *Rosa laevigata* (rosaceae) Biochem Syst Ecol. 52:23-26. DOI 10.1016/j.bse.2013.09.006

Yan X D, Wang Q M, Tie C et al (2017) Polydatin protects the respiratory system from pm2.5 exposure Sci Rep 7:40030. DOI 10.1038/srep40030

Yang B, Li J-J, Cao J-J et al (2013) Polydatin attenuated food allergy via store-operated calcium channels in mast cell World J Gastroenterol 19:3980

Yang B and Zhao S (2017) Polydatin regulates proliferation, apoptosis and autophagy in multiple myeloma cells through mtor/p70s6k pathway Onco Targets Ther 10:935-944. DOI 10.2147/OTT.S123398

Yang G, Fan L, Tian SJ et al (2017) Polydatin reduces il-1β-induced chondrocytes apoptosis and inflammatory response via p38 mapk signaling pathway in a rat model of osteoarthritis Int J Clin Exp 10:2263-2273

Yang J, Ou X, Zhang X et al (2017) Effect of different solvents on the measurement of phenolics and the antioxidant activity of mulberry (*Morus atropurpurea* Roxb.) with accelerated solvent extraction J Food Sci 82:605-612. DOI 10.1111/1750-3841.13638

Zamora-Ros R, Andres-Lacueva C, Lamuela-Raventos RM et al (2008) Concentrations of resveratrol and derivatives in foods and estimation of dietary intake in a spanish population: European prospective investigation into cancer and nutrition (epic)-spain cohort Br J Nutr 100:188-196. DOI 10.1017/S0007114507882997

Zeng Z, Chen Z, Li T et al (2015a) Polydatin: A new therapeutic agent against multiorgan dysfunction J Surg Res 198:192-199

Zeng Z, Chen Z, Xu S, Song R et al (2015b) Polydatin Alleviates Small Intestine Injury during Hemorrhagic Shock as a SIRT1 Activator. Oxid Med Cell Longev. DOI: 10.1155/2015/965961

Zeng Z, Chen Z, Xu S et al (2016) Polydatin protecting kidneys against hemorrhagic shock-induced mitochondrial dysfunction via sirt1 activation and p53 deacetylation Oxid Med Cell Longev. DOI: 10.1155/2016/1737185

Zhang H, Yu CH, Jiang YP et al (2012) Protective effects of polydatin from *Polygonum cuspidatum* against carbon tetrachloride-induced liver injury in mice PloS one 7:e46574.

Zhang J, Tan Y, Yao F, Zhang Q (2012) Polydatin alleviates non-alcoholic fatty liver disease in rats by inhibiting the expression of TNF-α and SREBP-1c Mol Med Rep 6:815-820.

Zhang M, Zhao Z, Shen M et al (2017) Polydatin protects cardiomyocytes against myocardial infarction injury by activating sirt3 BBA MOL BAS 1863:1962-1972

Zhang Q, Tan Y, Zhang N et al (2015) Polydatin supplementation ameliorates diet-induced development of insulin resistance and hepatic steatosis in rats Mol Med Rep11:603-610

Zhang W, Li Q, Zhu M et al (2008) Direct determination of polydatin and its metabolite in rat excrement samples by high-performance liquid chromatography Chem Pharm Bull 56:1592-1595

Zhang Y, Zhuang Z, Meng Q et al (2014) Polydatin inhibits growth of lung cancer cells by inducing apoptosis and causing cell cycle arrest Oncol Lett 7:295-301. DOI 10.3892/ol.2013.1696

Zhang Y, Li S, Wang W et al (2015) Beneficial effects of polydatin on learning and memory in rats with chronic ethanol exposure Int J Clin Exp Pathol 8:11116-11123

Zhang Z, Lu L, Liu Y et al (2016) Determination of antioxidants in *Smilacis glabrae* rhizoma by high-performance liquid chromatography with ultraviolet and mass spectrometry detection Analytical Letters 49:1975-1985. DOI 10.1080/00032719.2015.1133635

Zhao G, Jiang K, Wu H et al (2017) Polydatin reduces *Staphylococcus aureus* lipoteichoic acid-induced injury by attenuating reactive oxygen species generation and TLR2/NFκb signallingJ Cell Mol Med. DOI: 10.1111/jcmm.13194.

Zhao K, Jin C, Huang X et al (2003) The mechanism of polydatin in shock treatment Clin Hemorheol Microcirc 29:211-217

Zhao X, Li R, Liu Y et al (2017b) Polydatin protects against carbon tetrachloride-induced liver fibrosis in mice Arch Biochem Biophys 629:1-7

Zhou M, Chen X, Zhong D (2007) Simultaneous determination of trans-resveratrol-3-*O*-glucoside and its two metabolites in rat plasma using liquid chromatography with ultraviolet detection J Chromatogr B Analyt Technol Biomed Life Sci 854:219-223. DOI 10.1016/j.jchromb.2007.04.025

Zhou QL, Qin RZ, Yang YX et al (2016) Polydatin possesses notable anti-osteoporotic activity via regulation of opg, rankl and β-catenin Mol Med Rep14:1865-1869